RI 8567

Bureau of Mines Report of Investigations/1981

Evaluation of the Seismic System for Locating Trapped Miners

By John Durkin and Roy J. Greenfield

UNITED STATES DEPARTMENT OF THE INTERIOR

Report of Investigations 8567

Evaluation of the Seismic System for Locating Trapped Miners

By John Durkin and Roy J. Greenfield

UNITED STATES DEPARTMENT OF THE INTERIOR
James G. Watt, Secretary
BUREAU OF MINES
Robert C. Horton, Director

This publication has been cataloged as follows:

Durkin, John

Evaluation of the seismic system for locating trapped miners.

(Report of investigations / Bureau of Mines ; 8567)
Bibliography: p. 48-50.

1. Mine rescue work--Equipment and supplies. 2. Seismometers. I. Greenfield, Roy J. II. Title. III. Series: Report of investigations (United States. Bureau of Mines) ; 8567.

TN23.U43 [TN297] 622s [622'.8] 81-2170 AACR2

CONTENTS

ILLUSTRATIONS

ILLUSTRATIONS--Continued

TABLES

TABLES--Continued

EVALUATION OF THE SEISMIC SYSTEM FOR LOCATING TRAPPED MINERS

by

John Durkin[1] and Roy J. Greenfield[2]

ABSTRACT

This report discusses the configuration and system deployment for the postdisaster surface seismic system for detecting and locating trapped miners. It analyzes the results of 15 field tests to define a signal model, background noise levels, and subarray performance. A waveform modeling procedure is described and compared with observed waveforms. The resulting similarity indicates that the major factors affecting the signal amplitude, waveform, and spectral character are understood. A model is presented which gives the signal amplitude as a function of source type, source depth, and horizontal offset between source and receiver. Using this model a curve is presented which gives the range at which a signal will be detected for different signal and noise levels. Finally, and most important relative to the mission of the system, the ability of the system to detect signals on one or more subarrays is put into a probabilistic framework. For a strong source it is almost certain that a subarray directly over the source will detect the signal. After signal processing, it is highly likely that signals will be detected on sufficient subarrays to locate the trapped miner. Location errors have been found to be less than 100 ft in the majority of cases. Techniques have been used that can reduce the location errors to this level even when soil layer variation between subarrays is severe.

INTRODUCTION

Mine disasters continue to be a serious problem in underground mining. Disasters are caused by explosions, fires, cave-ins, or floods. Some explosions are so violent and extensive that they kill or suffocate, almost immediately, every man underground. However, if the men are not in the exact vicinity of the explosion and do not come in contact with the deadly gases following the fire, they may be rescued later.

[1]Supervisory electrical engineer, Pittsburgh Research Center, Bureau of Mines, Pittsburgh, Pa.

[2]Professor of geophysics, Geoscience Department, Penn State University, University Park, Pa.

Studies (15)[3] have shown that the men who barricade themselves to prevent the carbon monoxide from reaching them stand the best chance of survival. However, these men can be regarded as prisoners within the mine. Usual means of communication may be destroyed, prohibiting members of the rescue team from communicating with the trapped men. Without this communication the rescue team knows little about the condition of the men or their location. The last factor is the most regrettable, since reliable knowledge on the location of the entombed men could lead to prompt arrival of the rescue team and could prevent unnecessary deaths.

In 1970, the National Academy of Engineering (19) reported that a seismic system might be capable of detecting and locating trapped miners. They proposed that the miner would strike a part of the mine with any heavy object that could be found. The resulting vibrations would then be detected on the surface by the use of seismic transducers (seismometers), which will be referred to as geophones in this report. The vibrations are converted into electrical signals by the geophones and then amplified, filtered, and recorded. By comparing arrival times at several different geophone locations, the trapped miner could be located.

In 1971 Westinghouse Electric Co. (26) built and tested such a system. From 1972 until the present Westinghouse, in cooperation with the Mine Safety and Health Administration (MSHA) and the Bureau of Mines, has modified and tested the system in a variety of mines.

The purpose of this Bureau of Mines paper is to describe the present seismic system and to define its effectiveness in locating a miner trapped underground following a mine disaster. To predict the system's performance at a given mine, signal and noise models were formed from field test data, and signal detectability statistics were evolved. Results of the study indicated that this system should provide an effective means of locating trapped miners.

ACKNOWLEDGMENTS

The major portion of the field measurements used in this report were conducted by the Westinghouse Corp.'s Mine Emergency Operations Integrated Logistic Support group. Westinghouse personnel participating in the programs were Jim Moore, Ray Rouiller, Jerry Weinsert, Walt De Castro, John Frank, Herold Hannah, John Hartman, and Bob Koper. This field program was jointly funded by the Bureau of Mines and MSHA. Jeff Kravitz, of MSHA, was continually involved in the planning and execution of the field program.

Richard A. Watson and Wymar Cooper of the Bureau of Mines helped conduct the 1976 field tests.

Pennsylvania State University Department of Geosciences students who have made major contributions to the project were Mark Ruths, Jeff Hoffman, Pam Justice, Mark Angeleno, and Randy Christian.

---

[3]Underlined numbers in parentheses refer to items in the list of references preceding the appendixes.

SYSTEM DESCRIPTION AND OPERATION

System Deployment

Following a mine disaster in which it is believed that men are trapped underground and it has been determined that the seismic location system is necessary, the system is driven to or transported by cargo aircraft to the mine site. The system is then positioned over a known or suspected area of entrapment. Figure 1 shows the van housing of the seismic location equipment. Hopefully, this area is clear and easily accessible, but if not, it can be cleared by bulldozers and the system can be transported to the site by tracked vehicle or helicopter. It is recommended that to provide the best possibility of detecting and locating a trapped miner, the geophones be placed surrounding his most likely location. If the trapped miner is not within the area covered by the geophones he still may be detected and located, but accuracy in the calculation of his location may suffer (5). However, it is not necessary for the seismic van or its support equipment to be positioned within this area because of the large length of cable available to link the geophones to the van; also, wireless telemetry between the geophones and the van could be used. It is also recommended that the geophones be located away from any vehicle or personnel activity during attempted reception of seismic signals, because such activity could cause interference with signal receptions.

FIGURE 1. - Seismic van.

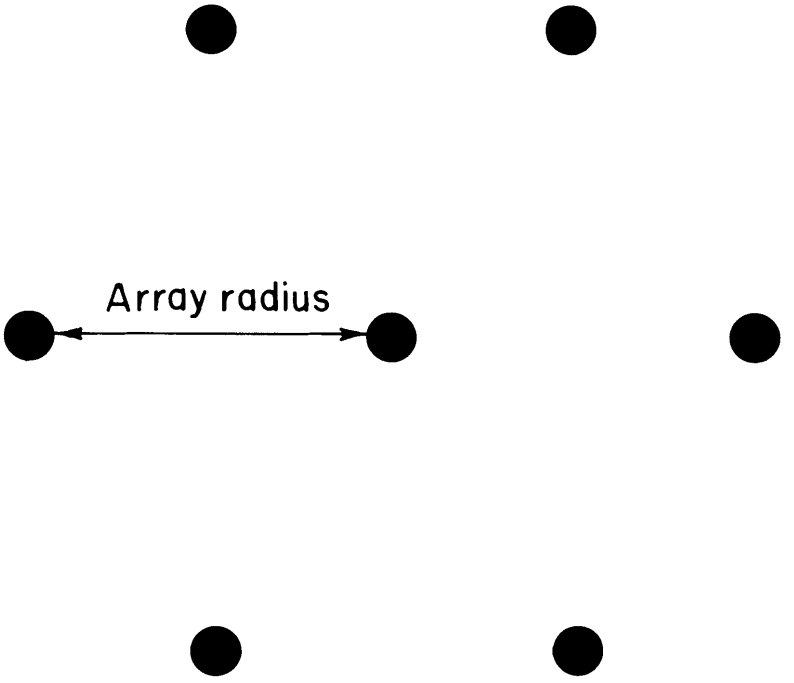

FIGURE 2. - Ideal array configuration.

After a site is chosen, the seismic array is deployed in a configuration that will cover the area to be monitored. An ideal array configuration is shown in figure 2. The array geometry is adjusted to the geometry of the mine and to surface conditions. The array consists of 7 subarrays; each subarray is composed of either 7 or 24 geophones configured as shown in figure 3. The detailed discussions of these subarrays are given in a later section. While the array is being deployed, a survey of the subarray locations is made using surveying equipment maintained with the seismic system.

MSHA has a continuing effort to explain to the mining community the operation of the seismic location system. The miner is instructed to do the following in the event he is trapped underground:

1. When all possible escape is cut off, the miner is to barricade himself for protection from possible toxic gases and wait for a signal from the surface, before attempting to signal the seismic system.

2. As soon as the system is in a state of readiness, the surface crew detonates three explosives which can be easily heard underground by the trapped miner.

3. After hearing these 3 shots, the miner is to pound 10 times on a part of the mine, preferably the roof or a roof bolt, with any heavy object he can find; a heavy timber is best. Figure 4 shows the miner pounding while an operator in the seismic van listens for the miner's signal.

4. Following this the miner is to rest 15 minutes and listen for five shots from the surface which will indicate to the miner that his signal has been heard and help is on the way.

5. If the miner hears no shots, he repeats signaling every 15 minutes.

During the expected signaling period, attempts are made to reduce surface activity while the seismic system is in use to optimize the chances of detecting the miner's signal. This system operates continuously, but this quiet period should enhance the chances of detection during the expected signaling period.

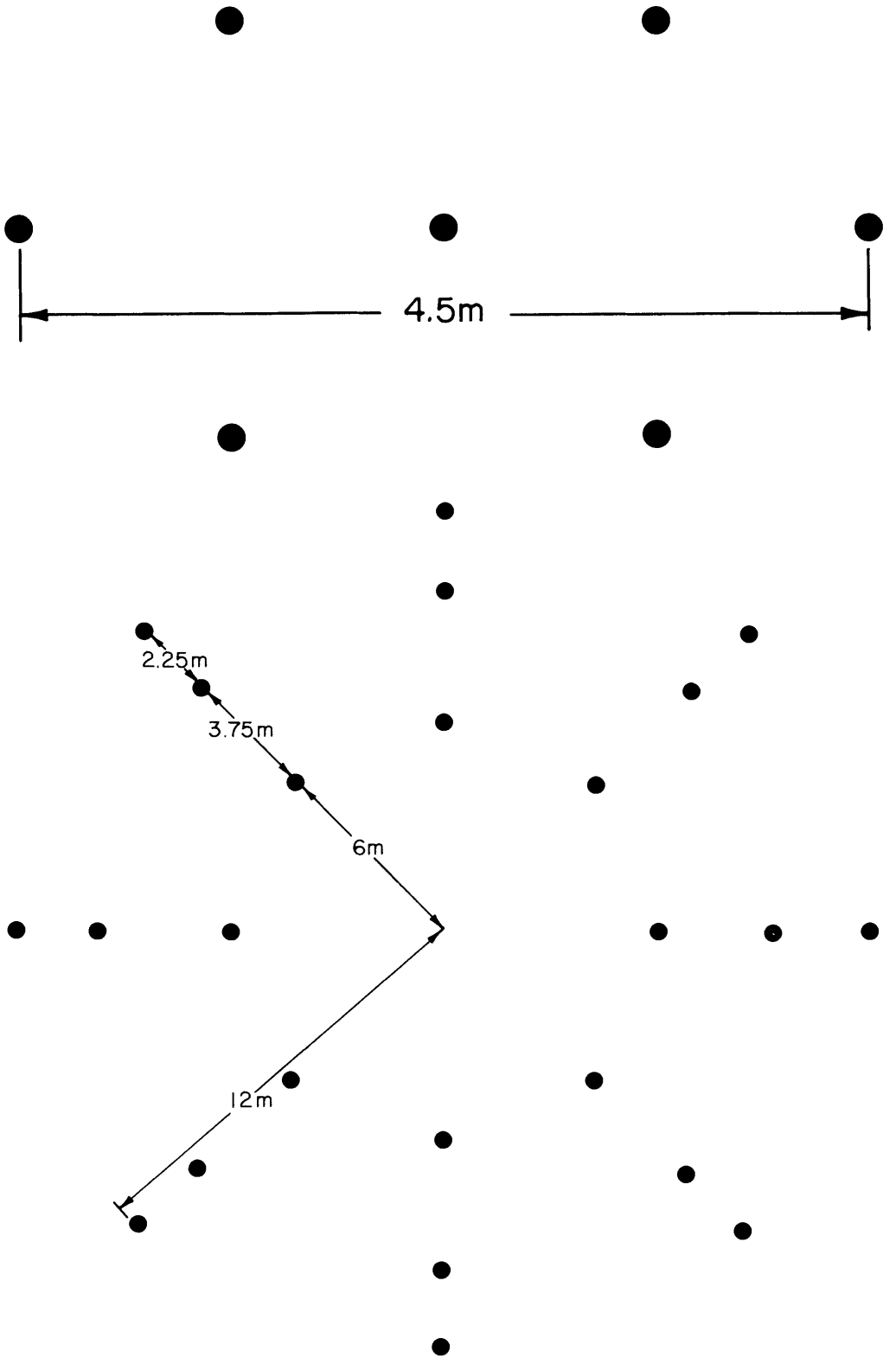

FIGURE 3. - Subarray configurations of 7 geophones (top) and 24 geophones (bottom).

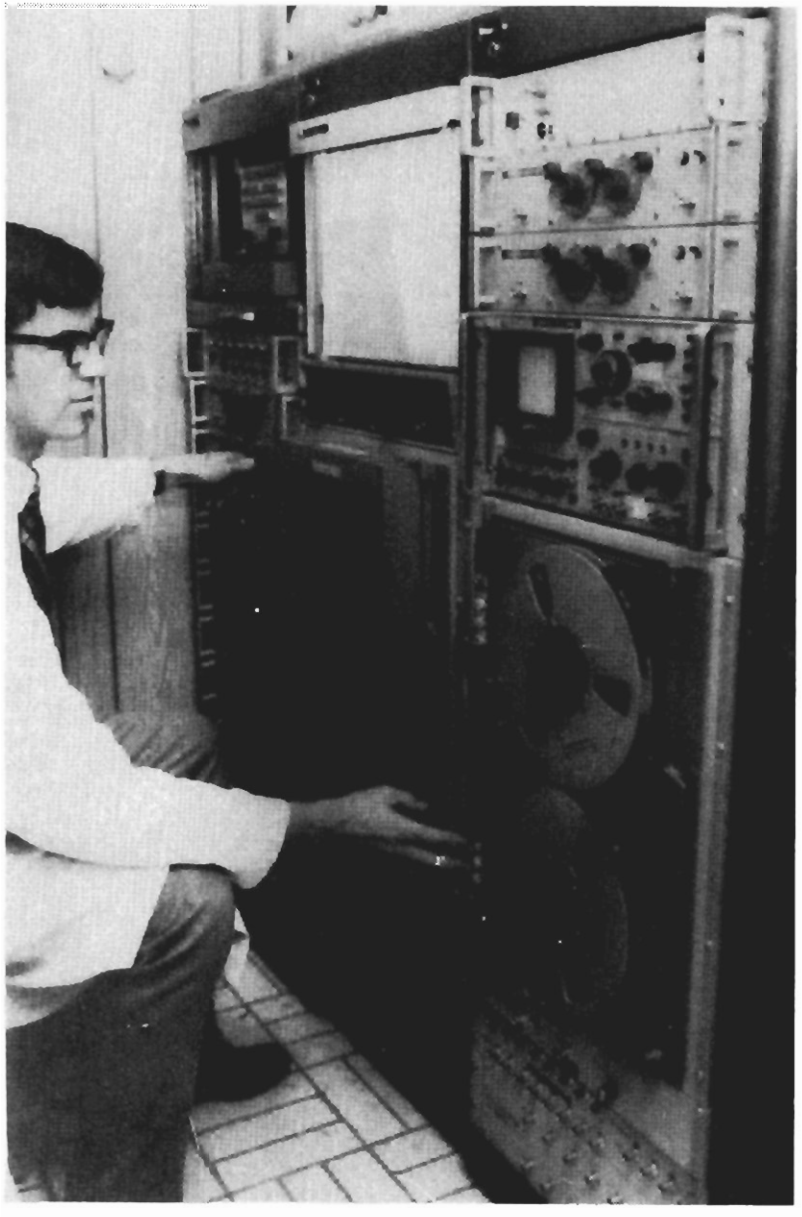

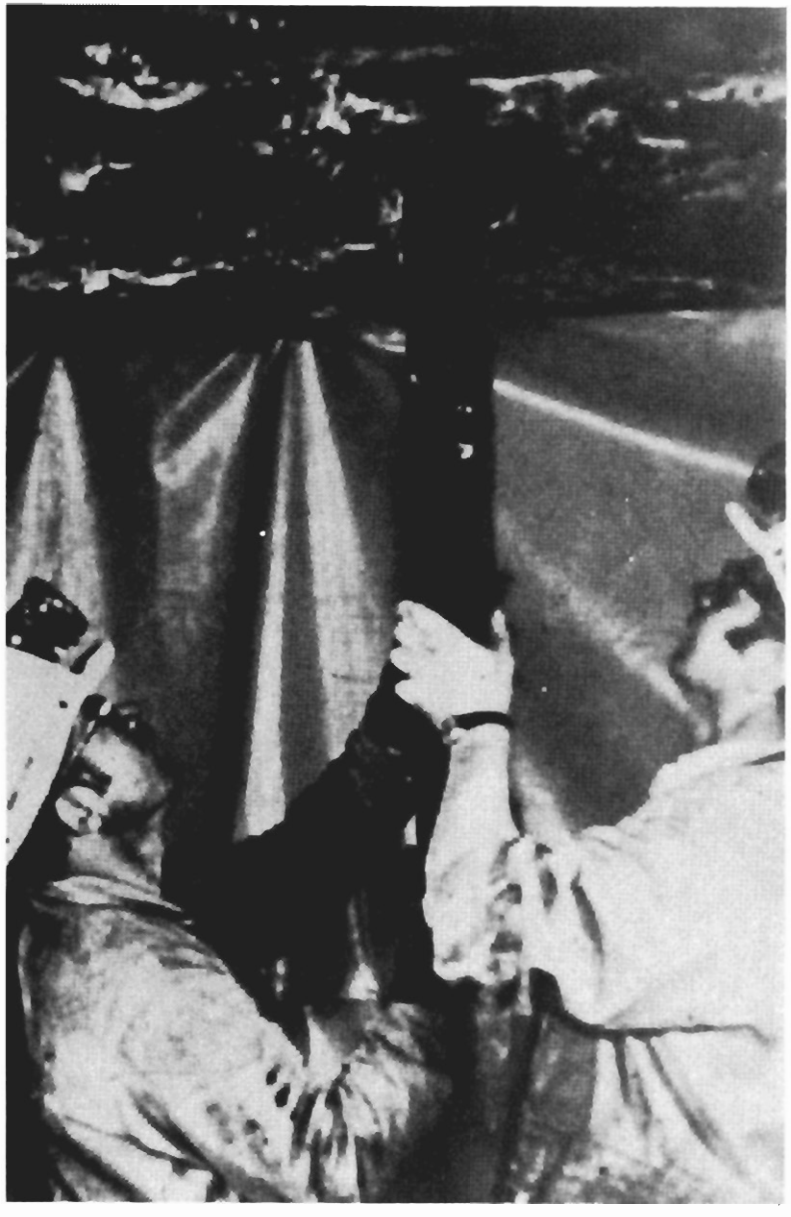

FIGURE 4. - Miner pounding while surface personnel listen for signal.

Once the signal is detected and miner's location has been determined, directions are given to the rescue team to guide them in their rescue efforts. If a rescue team is unable to reach the trapped men, a drilling rig is positioned over the site of the miner's location and a rescue borehole is drilled for his evacuation.

System Instrumentation

The operation of the system can best be described by referring to the system diagram shown in figure 5. The geophone used is the Geospace[4] GSC-11D model M-3, having a natural undamped frequency of 14 Hz, a coil resistance and shunt resistance of 4,000 ohms, and an intrinsic sensitivity of 2.95 V/in/sec. At each subarray a preamplifier increases the signal level and sends it to the van via cable or radio telemetry. At the van the signals are first each passed separately through a tracking digital notch filter. This filter removes narrow-band manmade interference such as power line pickup or seismic disturbances caused by local machinery by latching onto the fundamental frequency of interference and tracking it if slight variations in frequency occur. The filter also removes the harmonics of the interfering noise. This initial processing step eliminates interference that would, in some instances, limit the system performance.

An example of the performance of this filter can be seen in figure 6. Figure 6A shows a seismic record heavily contaminated with 60-Hz interference.

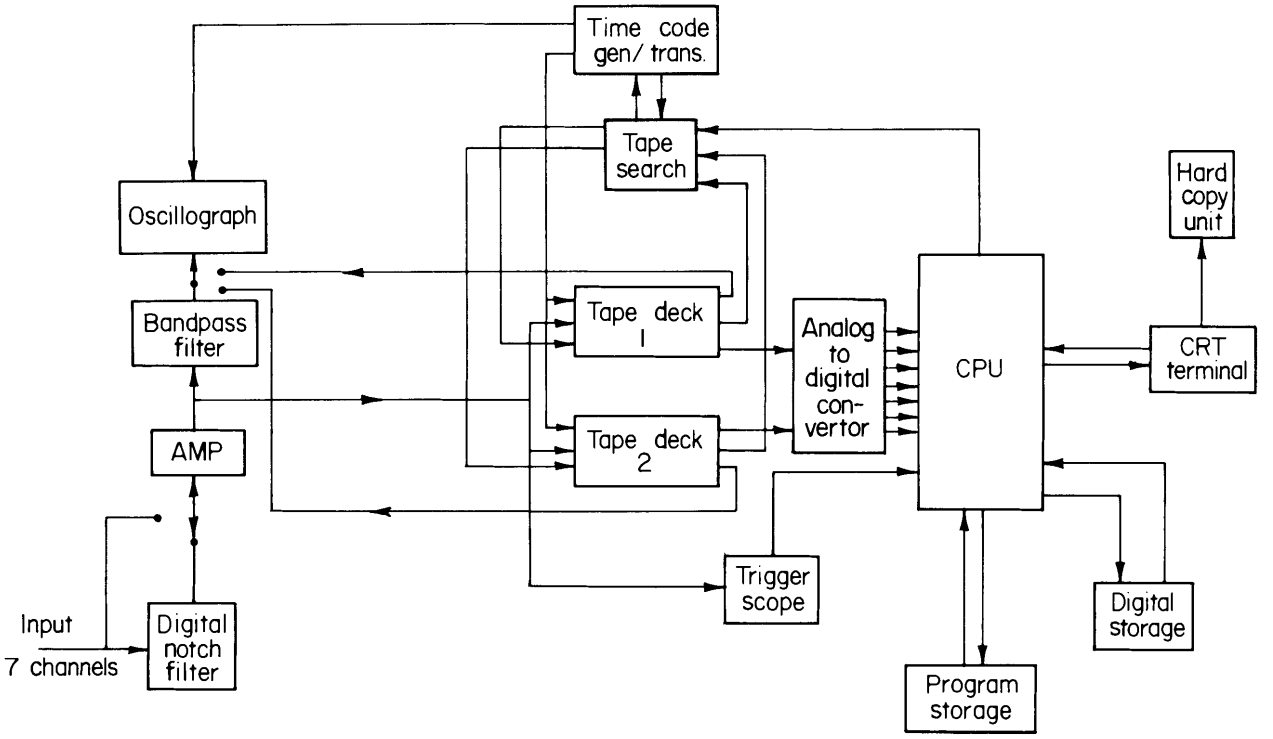

FIGURE 5. - Seismic system block diagram.

[4]Use of brand names is for identification purposes only and does not imply endorsement by Bureau of Mines.

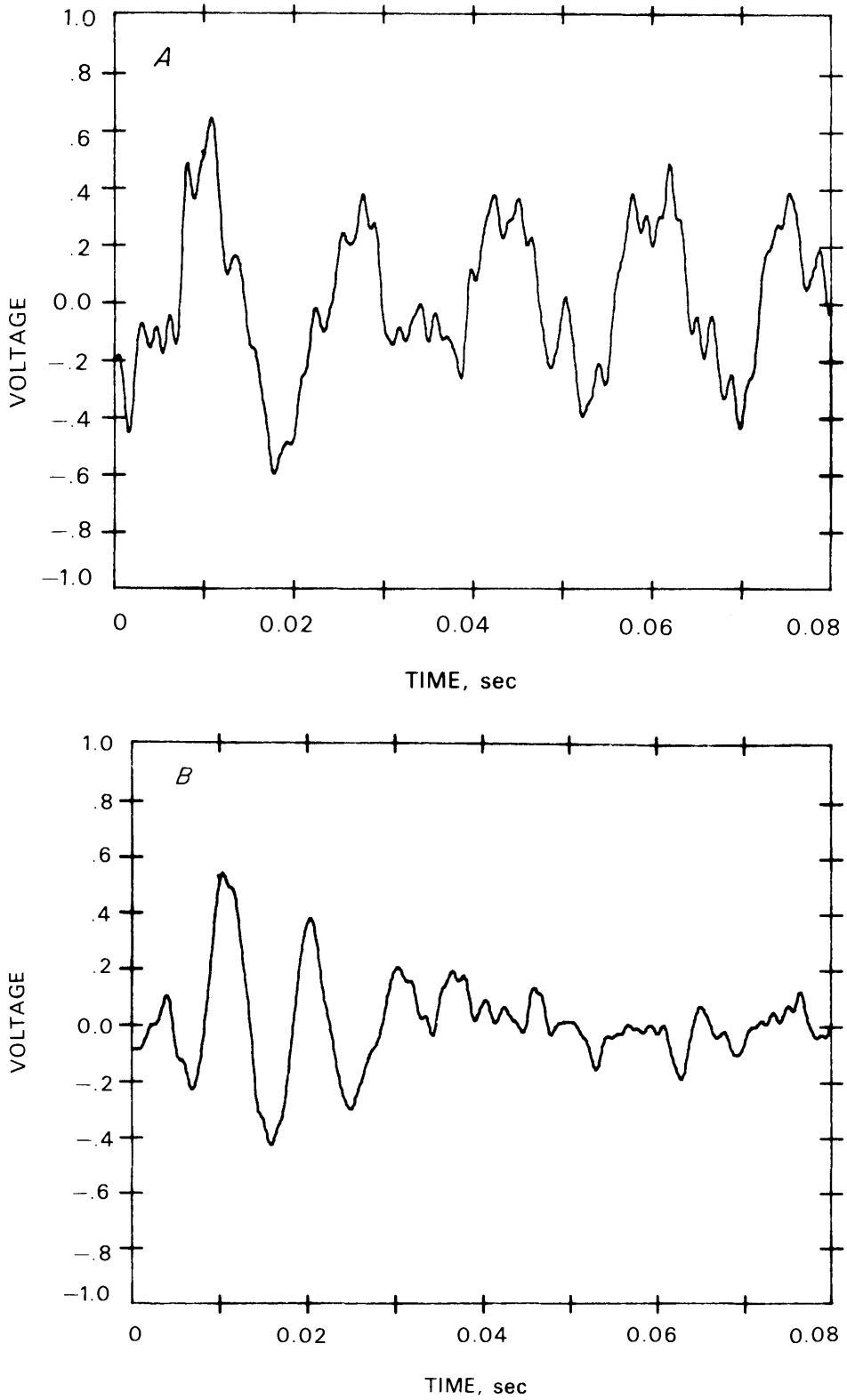

FIGURE 6. - Seismic record showing signal and noise (*A*) before digital notch filtering and (*B*) after filtering.

Figure 6B shows the same record after passing through the notch filter and illustrates how a miner's signal is easily seen after filtering, whereas prior to filtering it would be impossible to see the signal.

After notch filtering the signals are amplified and then recorded on analog tape. The signals are bandpass-filtered 20 to 200 Hz and displayed on an oscillograph record for recordkeeping purposes. By visually monitoring the oscillograph record, the operator can determine whether a signal has occurred.

When the operator detects a signal, the analog tape containing the event is replayed into a PDP 11/34 computer via an analog-digital (A-D) converter. The computer performs interactive signal processing on the data and displays the results on the CRT terminal. A permanent record can be obtained using the hard copy unit.

One commonly used signal-processing technique is known as stacking. Here the pulses from the subarray with the strongest signal are time-alined and added. In theory, this leads to an increase of $\sqrt{N}$ in amplitude signal to noise ratio (SNR), where N is the number of pulses stacked. In practice, this $\sqrt{N}$ improvement is in fact normally obtained. Stacking can thus provide an advantage for channels where the pulses cannot be seen to obtain arrival times. Using time differences between pulses obtained from the stronger channel, stacking can help in detecting the pulses buried in the noise on the weaker channels.

When the processing has been completed, the relative arrival times of the signals from each channel are determined. These data, together with information on the location of the subarray and the velocity of seismic waves obtained by refraction surveys, are submitted to the computer location program to determine the miner's location.

The present system relies on the operator's ability to determine when a signal has occurred. Manual detection of the signal can be unreliable due to the low SNR often encountered and the inability of the operator to maintain peak performance over extended periods. At present, efforts are being made to automatically detect the miner's signal by computer, thus eliminating possible human error.

SEISMIC NOISE

Seismic noise can be a major problem when detecting small seismic signals. Since the signal level from a trapped miner can be on the order of a few micro-inches per second (μips), normal background noise may mask the signal. Thus, information is needed on the types of noise sources, the amplitude ranges, and the amplitude variation with frequency and time.

Typically, in the field three common noise sources are encountered: (1) Natural seismic background noise, (2) man-made seismic noise, and (3) man-made electromagnetic interference (EMI) coupled into the field equipment. Narrow-band man-made noise can be eliminated through digital notch filtering techniques previously discussed. Thus, in this report we will be mainly

concerned with natural seismic noise that is not of very narrow bandwidth and that cannot be attributed to an obvious manmade noise source.

Since seismic noise tends to vary widely as a function of time, geographic location, and frequency, it is not possible to make precise predictions of the noise at the site of some future mine disaster; thus the noise can be treated only in statistical terms. For some purposes, however, it is sufficient to know the noise characteristics within fairly broad limits.

Study of the miner-induced seismic signal spectra indicates that most of the signal energy can be found in the frequency band between 20 and 200 Hz. Therefore, discussions on seismic noise will be for noise found within this band.

The noise data used in this study were from Frantti (9-10), field studies at 12 mines by Westinghouse (24), and a field study by the Bureau of Mines at 3 different mines. In each of these studies the noise in the band of interest had a roughly $1/\sqrt{f}$ frequency dependence.

The spectra of earth noise in the frequency range 0.2 to 100 Hz were measured by Frantti in one-third octaves at a number of locations within the United States and at other North American and foreign sites. In the reduction of the data, attempts were made to delete records containing obvious manmade noise. Frantti gave curves of maximum and minimum values of peak-to-peak (P-P) ground velocity up to 100 Hz. These curves generally show a well-behaved $1/\sqrt{f}$ relationship with frequency. Using this relationship, the spectrum was extrapolated to 200 Hz.

Studies have shown that the amplitude of the envelope of seismic noise is often Rayleigh distributed (4). Based upon this assumtion Frantti's data are then converted to root mean square values (rms) in the manner shown in appendix A. The high and low values of seismic noise found by Frantti are shown in table 1.

TABLE 1. - Seismic noise, μips (rms)

Test data	Average	High	Low
Westinghouse.....	1.10	8.00	0.17
Bureau.....	1.00	2.00	.30
Frantti.....	NAp	14.00	.37
Greenfield.....	NAp	2.55	.37

NAp Not applicable.

These results provide information only on the extreme bounds of seismic noise. A more meaningful presentation of Frantti's work has been given by Greenfield (13). Here seismic noise rms levels are given where these levels are exceeded 75 pct of the time (low noise) and 25 pct of the time (high noise). Greenfield's results are for the frequency range of 25 to 100 Hz. Using the fact that the seismic noise varies as $1/\sqrt{f}$ in frequency, these results are adjusted to include the band 20 to 200 Hz. The resulting high, low, and average values found are shown in table 1.

The Bureau of Mines performed field tests at three midwestern coal mines. A number of noise samples were taken. The obvious manmade noise was eliminated, and the natural background noise was averaged over a 1-minute period. Results are shown in table 1. The spread in this data is much less than the spread found in the Frantti data and may be explained by the much smaller data base used by the Bureau. However, the average noise level appears to be near the midpoint found between the boundary curves of Frantti.

Westinghouse (24) performed field tests to evaluate the performance of the trapped miner seismic system. Tests were performed at 12 mines in the Southern Appalachian, Midwestern and Far Western, and mid-Appalachian regions. At each mine noise data were taken at various times and locations using seven geophones connected in parallel. Results once again are shown in table 1.

To some degree the Westinghouse noise levels are artificial. These noise levels do not represent true natural background noise levels since the seven-geophone subarray used reduces the noise level relative to a single geophone. Typical expected values of noise reduction for this subarray are 2 to 8 db (6). In the data reduction done by Westinghouse, no attempts were made to delete manmade noise sources because this data reduction was performed in the field by measuring the noise levels from a visicorder display, and no processing capability was available at the time to remove the manmade interference. Studies performed on a few tapes indicated the true natural noise levels were reduced by 4 to 8 db when the manmade noise was eliminated. To some extent these two opposing influences, subarray noise reduction and manmade contamination, tend to cancel one another, so the levels of noise reported by Westinghouse should approximate natural ground motion on a single geophone. Finally, in many instances, the data appeared to be thermal noise limited; thus caution is advised in using the minimum level for the Westinghouse data.

THEORETICAL SEISMIC WAVEFORM MODELING PROCEDURE

An analysis was performed to understand the factors that affect the seismic signal amplitude, waveshape, and signal spectra. Based on this analysis a waveform modeling procedure (WMP) was developed to model seismic signals generated from impacts on the surface of mine openings. The output of the WMP is the predicted vertical particle velocity of the surface geophone, denoted by V_e. This procedure was implemented in a Fortran computer program and is shown in figure 7. The computations for each of the boxes are convolved to give a final theoretical waveform, which is then compared with forms recorded on field tests.

A major factor that determimes the seismic waveform is the time history of the force g(t) that the miner's implement (for example, timber) applies to the mine roof or floor. Measurements of this time history are not available, so a theory was developed to give g(t). The theory begins by calculating the momentum, P, that the implement has at the time it contacts the roof, as shown in figure 8. Let a man apply an upward force, F, to the implement of mass, M, over a distance, D. From simple physics the velocity of the mass at impact will be $\sqrt{2(F-MG)D/M}$. The term MG reduces the upward applied force F by the gravity force MG, G being the gravitational constant. Thus the momentum is

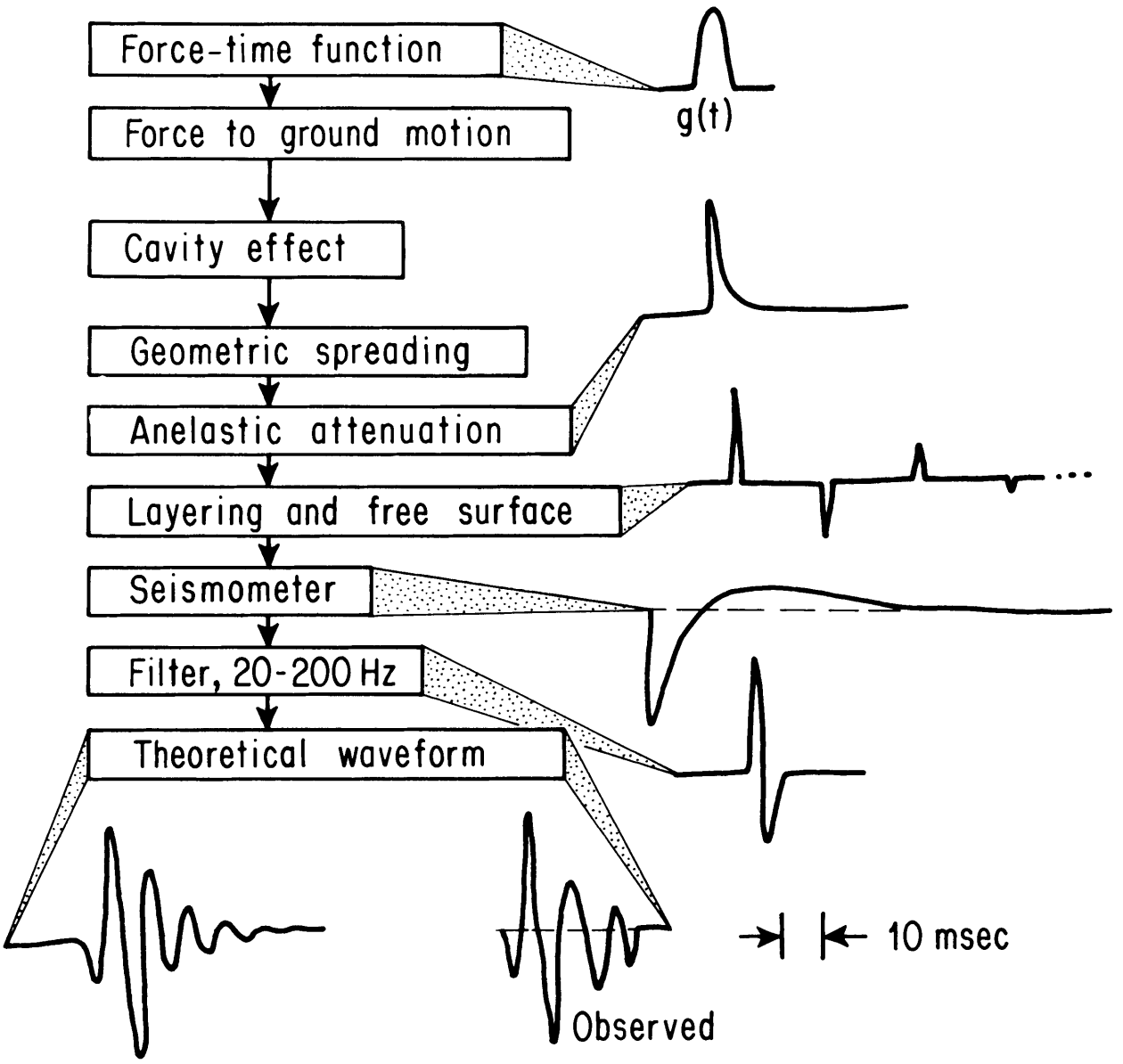

FIGURE 7. - Flow chart of waveform modeling procedure.

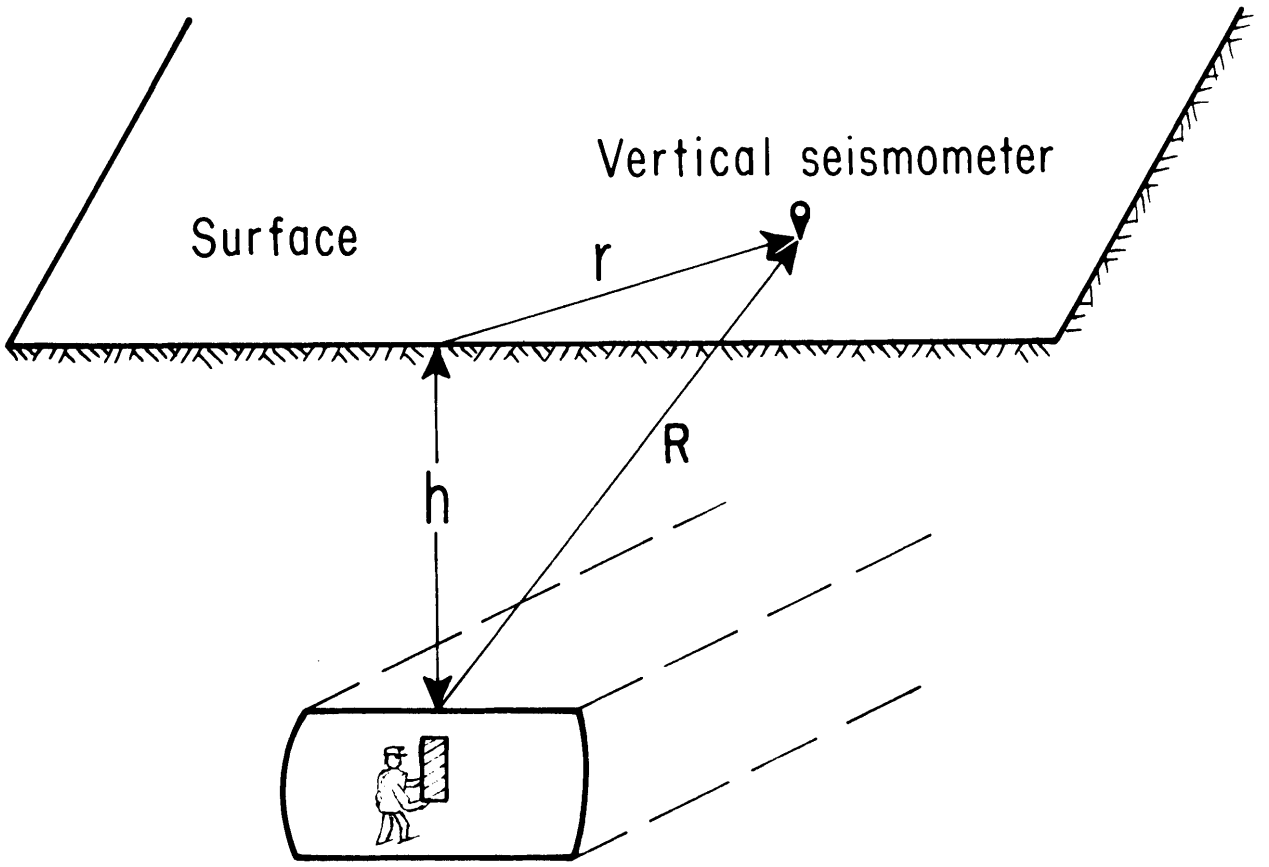

FIGURE 8. - Man signaling with timber on roof of mine.

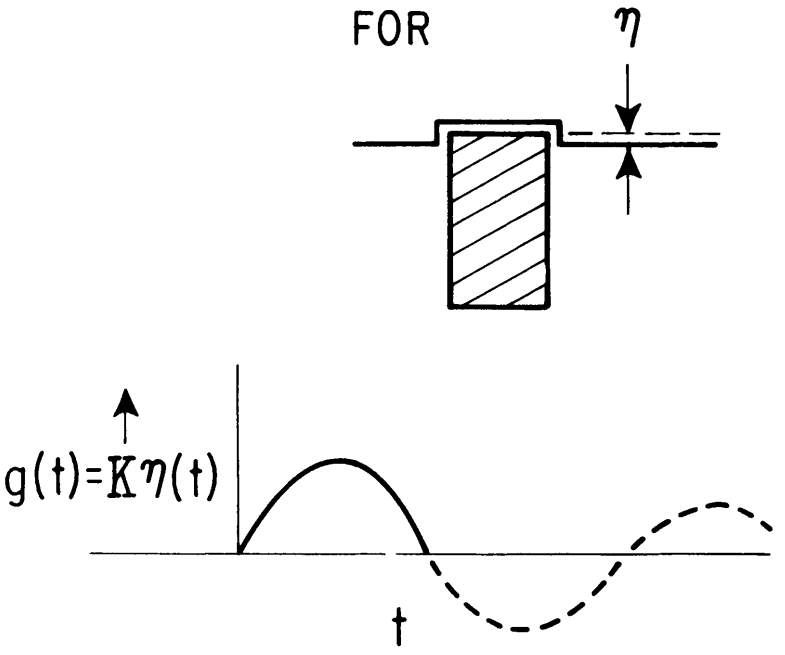

FIGURE 9. - Surface force-time function.

$P = \sqrt{2M\,(F-MG)\,D}$. Note that if $F >> MG$, the momentum is $P = \sqrt{2MFD}$, which predicts a roughly $\sqrt{M}$ dependence for momentum.

It can be shown based on work by Sung (23) that if the wavelengths involved are long compared with a length characterization the surface area of the implement that is in contact with the surface of the mine opening, then the force the implement exerts on the surface is proportional to the amount the surface is displacing $\eta(t)$; see figure 9. The force is then written as $g(t) = K \cdot \eta(t)$. Here K is the constant relating the

surface displacement and the source applied to the surface of the mine opening. If the timber were to remain in contact with the surface it would undergo a harmonic motion of the form

$$\eta(t) = \eta_o e^{-\alpha t} \sin \frac{\pi t}{\tau_s/2} . \tag{1}$$

Here τ_s is the period of the surface force. This form was suggested previously by Quo (21). However, after the first half cycle, which is shown as the solid line in figure 9, the implement will separate from the surface. In physical terms it will bounce off. The decay constant, α, is small, so only a small decay will occur during the first half cycle. Thus, for practical purposes g(t) is of the form

$$g(t) = \begin{cases} g_o \sin \frac{\pi t}{\tau_s/2} & 0 \leq t \leq \tau_s/2 \\ 0 & \text{otherwise} \end{cases} . \tag{2}$$

$\tau_s/2$ is the dwell time that the implement is in contact with the surface. A theory has been developed that relates τ_s to the elastic constants of the surface and to M. If the contact is a 0.1-m-radius disk, the predicted value for τ_s is less than 1 msec. Results to be discussed below indicate that the actual value of τ_s is much longer, about 10 msec. Thus, it is probable that when hitting a roof bolt or floor, a much smaller area than the whole of the end of the implement makes contact with the surface; this will give a longer τ_s. Therefore, it is not believed that τ_s can presently be predicted theoretically, and it is treated as an adjustable parameter in the WMP. It would be useful to have measurements of τ_s.

The value g_o is obtained from a momentum argument. The upgoing momentum is P, and the implement bounces off with a downward momentum εP, where $0 \leq \varepsilon \leq 1$. Thus the momentum change in the implement is $(1 + \varepsilon)$ P and must be equal to the time integral of g(t).

$$P(1 + \varepsilon) = \int_0^{\tau_s/2} g(t)dt = g_o \int_0^{\tau_s/2} \sin \frac{\pi t}{\tau_s/2} dt, \tag{3}$$

which gives

$$g_o = \frac{\pi}{\tau_s} (1 + \varepsilon) \cdot \sqrt{2 M(F - MG) D}. \tag{4}$$

This completes the definition of the force time function.

Returning to the geometry shown in figure 8, the outgoing P-wave radial displacement is next related to the force-time function. White (27) gives the radial displacement (good at more than a few wavelengths from the source) as the equation

$$d_R(t) = \frac{\cos \Theta}{4\pi\rho R V_p^2} \cdot g(t - R/V_p), \tag{5}$$

where Θ is the angle between the source-to-receiver direction and the vertical, ρ is the density, R is the source-to-receiver distance, and V_P is the P-wave velocity. This expression is for a point source in an infinite medium. A blow on the roof is assumed to be an upward force and a floor blow a downward force. To include the effect of the mine tunnel or cavity, the theory described by Greenfield (14) is used. The geometric spreading is given for the present situation by the 1/R term in equation 5. The effect of an elastic attenuation (often called Q-damping) on the wave as it propagates is included by using the Futterman (11) operator. The effect of geologic layering and the free surface of the earth is included by the method developed by Haskel (16), using a modification of the program described by Leblanc (18). The transfer function between the ground displacement and the voltage output of the seismic sensor was calculated based on the description of a seismometer given by Bollinger (2). The seismic system 20- to 200-Hz filter response was obtained by recording the impulse response of the filter.

Figure 10 shows the cavity and geologic model used in computing the seismograms to be described. The mine is included as an 8-m-diameter horizontal cylindrical opening. The diameter was taken to approximate the width of a mine opening. The rock P-wave velocity was taken as 3,000 m/sec, which is typical of the normal mine overburden. The soil layer P-wave velocity used was 1,000 m/sec. The soil thickness is denoted by D_s.

The waveforms given by the WMP give extremely good fits to records observed at the mine field tests. Both the waveshapes and absolute amplitudes are well fit. The first example is from the Orient #6 Mine; figure 11 shows the seismograms and figure 12 the spectrum. The parameters used in constructing these and the other theoretical waveforms are given in table 2. The lower spectral content of the signal from the Orient #6 floor blow is due to a larger τ_s, probably caused by soft floor material; also, the higher frequencies generated by the source are shielded by the mine opening. A second example, from the King Mine, is shown in figure 13. In figure 14 the signals from an event at the Orient #6 Mine are shown. Also shown are the observed amplitudes and the amplitudes predicted by the WMP. Notice that the WMP is able to predict the variation of amplitudes between subarrays for this event.

TABLE 2. - Parameter values used in waveform modeling procedure

Parameter	Rock	Soil
P-wave velocity.....m/sec..	3,000	1,000
S-wave velocity.....m/sec..	1,732	350
Density.....g/cm^3..	2.5	1.6
Cavity diameter.....m..	8	NAp
Source depth.....ft..	800	NAp
Q (Quality factor).....	30	NAp

NAp Not applicable.

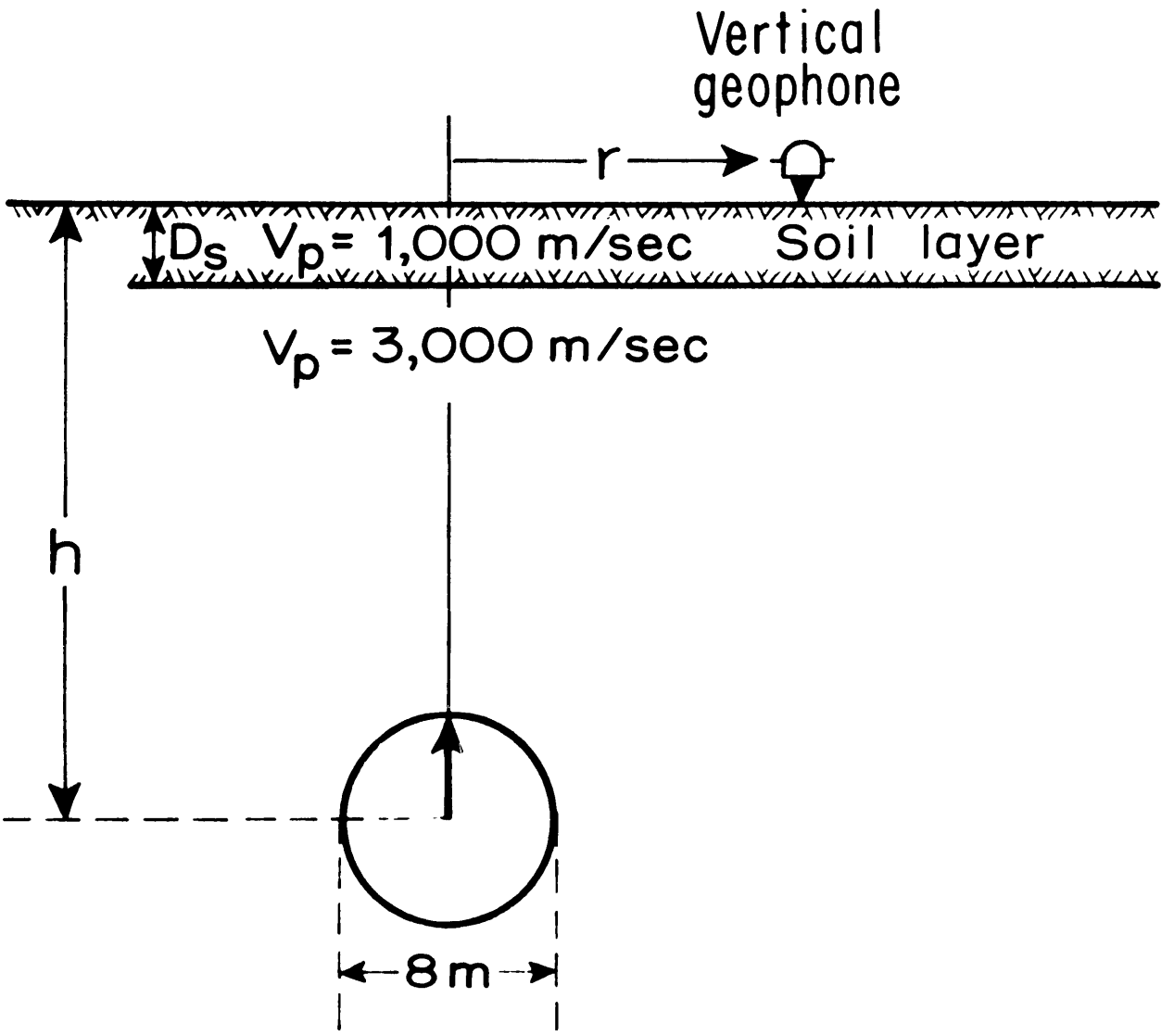

FIGURE 10. - Geometry and parameters used in waveform modeling procedure.

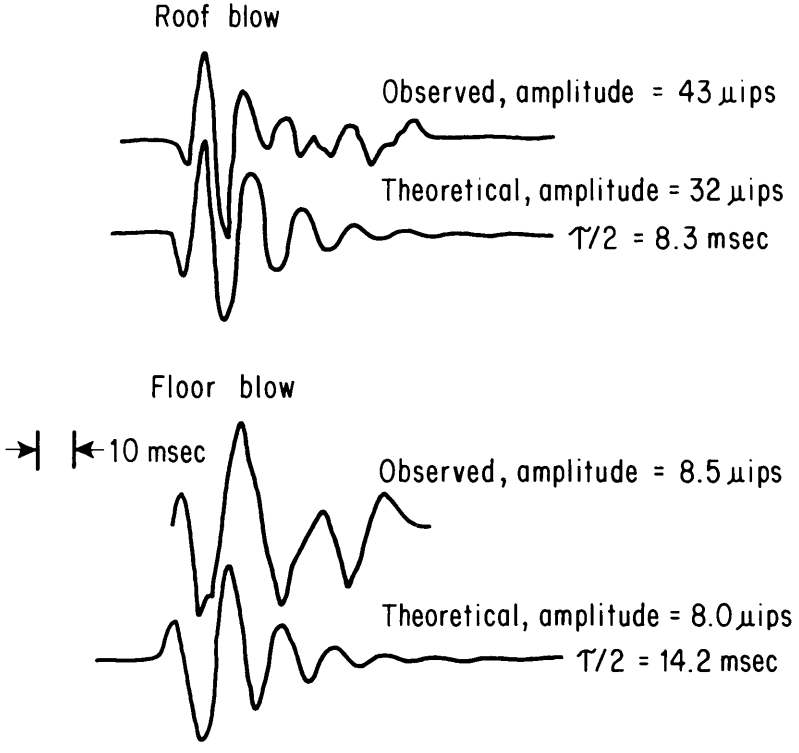

FIGURE 11. - Comparison of observed and theoretical seismograms at ~800-ft depth, Orient #6 Mine.

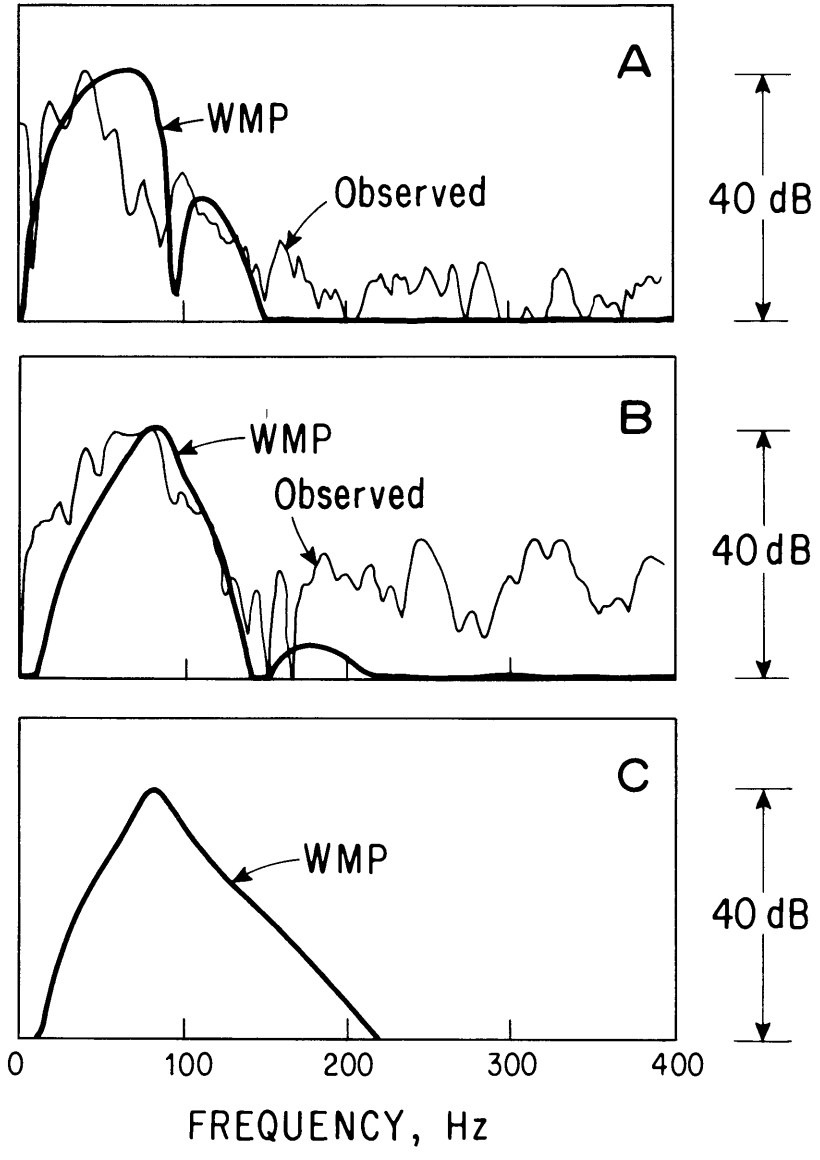

FIGURE 12. - Spectrum of Orient #6 data compared with spectrum from WMP. *A*, floor blow, $\tau_s/2 = 14.2$ msec; *B*, roof blow, $\tau_s = 8.3$ msec; *C*, WMP only with $\tau_s/2 = 5.0$ msec.

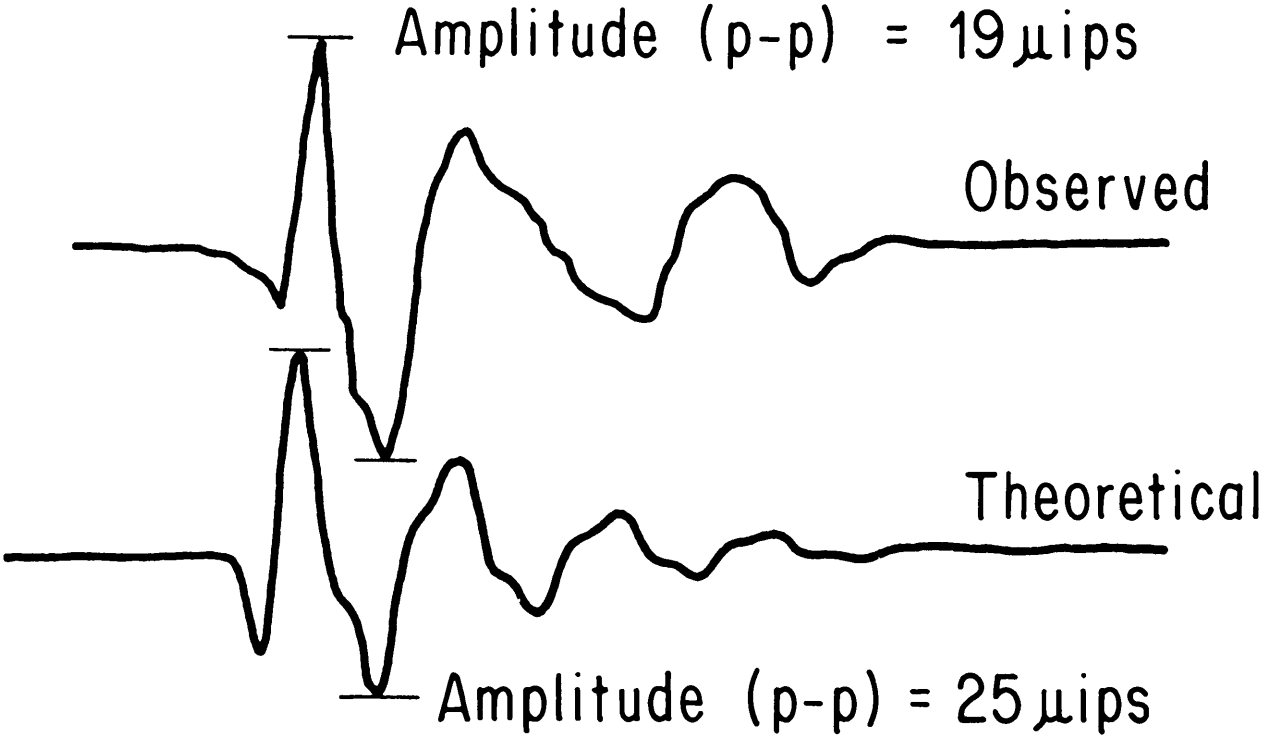

FIGURE 13. - Comparison of observed and theoretical seismograms at 1,800-ft depths, King Mine.

Figure 15 shows the effect on the waveform of soil thickness. For no soil, (D_s = 0 m) the waveform is a single simple pulse. For a thick soil layer (20 m) the waveform is a series of pulses of decreasing amplitude. These represent the successive wave bounces between the surfact and the soil-rock interface. The time between pulses is the two-way travel time in the layer. As the layer thickness decreases, the time between pulses decreases; when D_s is reduced to 10 m the pulses overlap in time.

The exact form of the signal is quite dependent on the D_s. The signals for D_s values from 2.5 m to 10 m resemble the actual waveforms from field tests, but the single simple pulses do not. This indicates that a soil layer was present at the mine sites. This is in agreement with seismic refraction results at the mine sites.

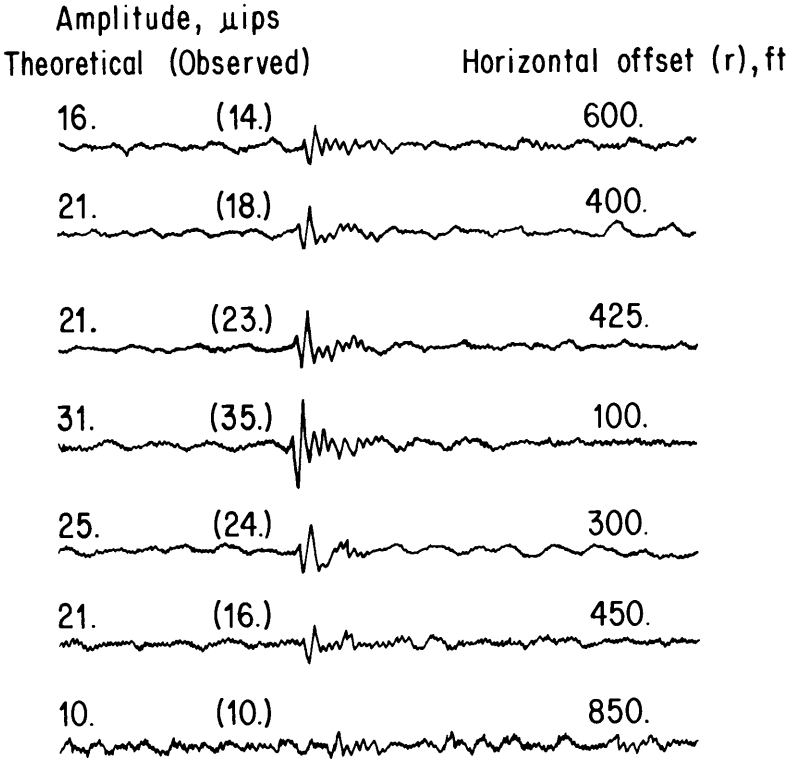

FIGURE 14. - Comparison of observed and theoretical amplitudes at ~800-ft depth, Orient#6 Mine.

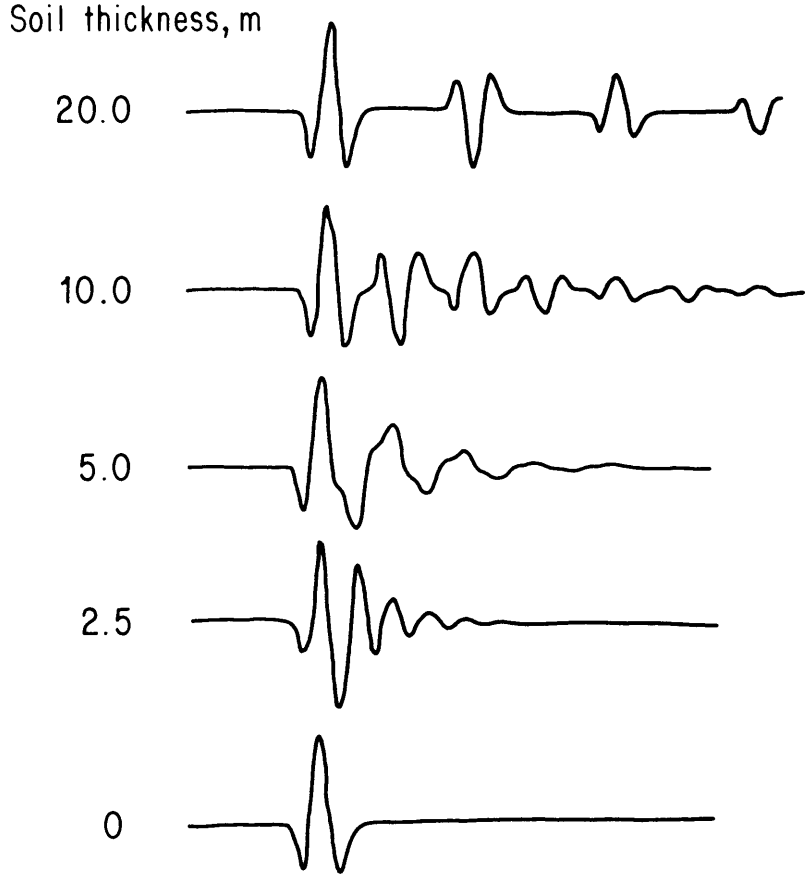

FIGURE 15. - Effect of soil layer thickness on vertical seismograms.

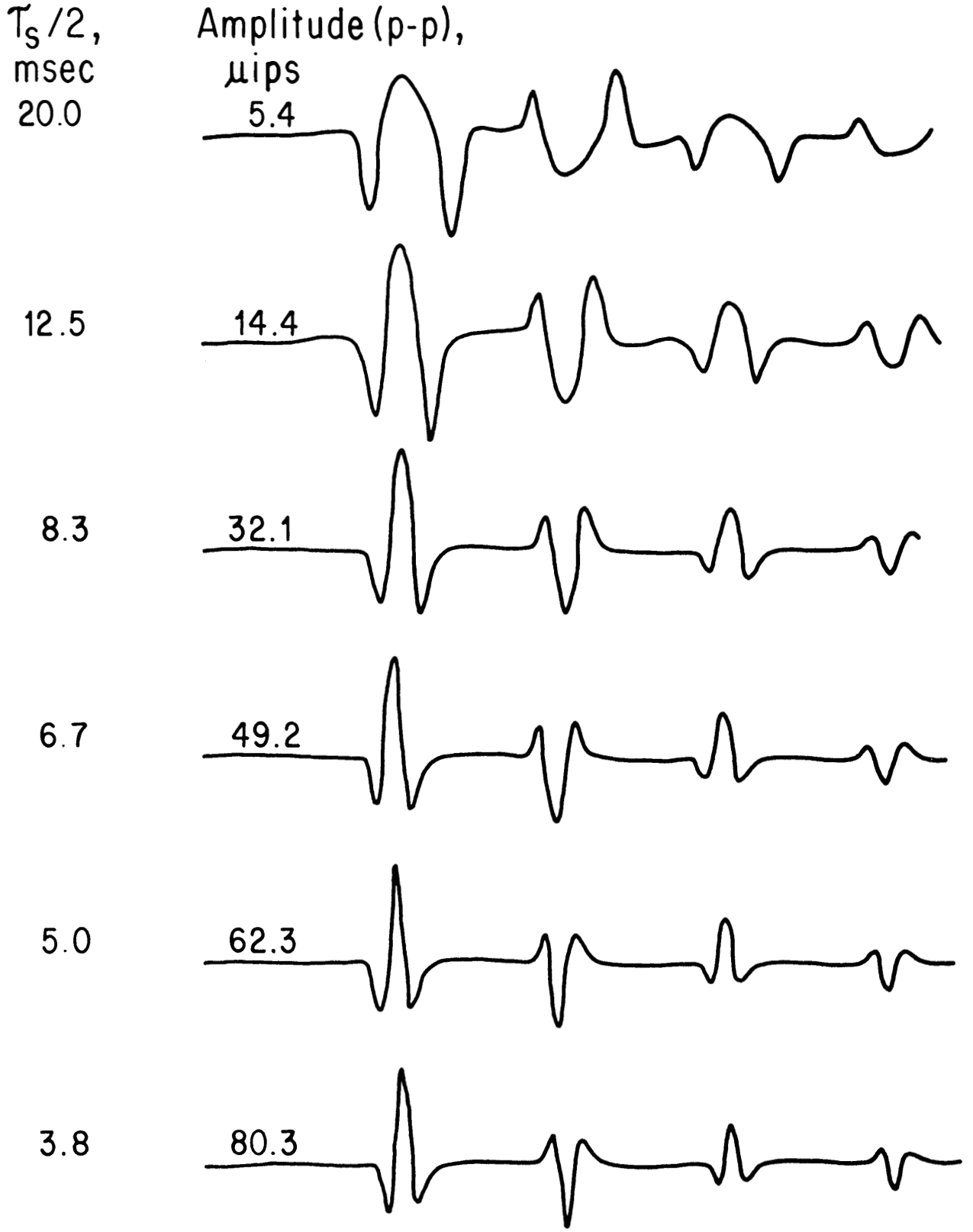

FIGURE 16. - Effect of force pulse width, $\tau_s/2$.

The P-P amplitude of the first cycle or so is not dependent on the soil thickness if the soil thickness is great enough for the first pulse to develop before the second arrives.

Finally, the effect on the signal caused by varying τ_s is shown in figure 16. A soil thickness of 20 m was used for this figure to allow examination of the change in the simple pulse shape. As expected, the pulses appear longer for the larger τ_s. It can also be noticed that the amplitude of the pulses increases with decreasing τ_s. The amplitude dependence is approximately $(1/\tau_s^2)$. Thus the variation of τ_s is a major factor that contributes to the scatter of amplitudes in the field test data. Since τ_s decreases as the surface being struck becomes more rigid, the signal amplitude should increase with increasing surface rigidity.

SIGNAL AMPLITUDE MODEL DERIVED FROM FIELD TESTS

The following discussion is divided into two parts. In the first part, an extensive set of data taken from three coal mines in Kentucky in 1976 is discussed. For these data a large timber on a roof bolt source gave the largest signal, and impacts from this source were used to develop a mathematical form for a model of signal strength. In the second part, signal amplitude data from 12 field tests conducted in 1977 are analyzed using the form of the signal model from the first part. For these data the signals from the best application point at each mine were used since at some mines no roof could be hit.

1976 Kentucky Coal Mines Results

The most extensive data reduction was done on data from 1976 field tests at three Kentucky coal mines: Peabody Camp No. 1, Island Creek Hamilton #1, and the Freeman-United Orient #6. These data were used to find the best form for the representation of the dependence of signal amplitude on the mine depth, h, and on the horizontal offset between source and receiver, r (fig. 17).

The data used to develop this model consisted of signals from large-timber blows on roof bolts as measured with the seven-geophone, 15-ft-diameter subarrays. Large-timber blows on roof bolts consistently gave larger signals than other sources at these mines. The signal amplitude is defined as the P-P value of the ground velocity, V_e, in units of microinches per second.

Using theoretical considerations, three forms were initially tested to see which fit the data best. They were

$$V_e(k,r) = \frac{A_M}{R} \cos^M \Theta \qquad (6)$$

with $M = 0$, 1, or 2.

$$Ve = \text{Peak-to-peak ground velocity, } \mu ips$$
$$= A_1 \cos\theta / R$$
$$A_1 = Ve \cdot R / \cos\theta$$

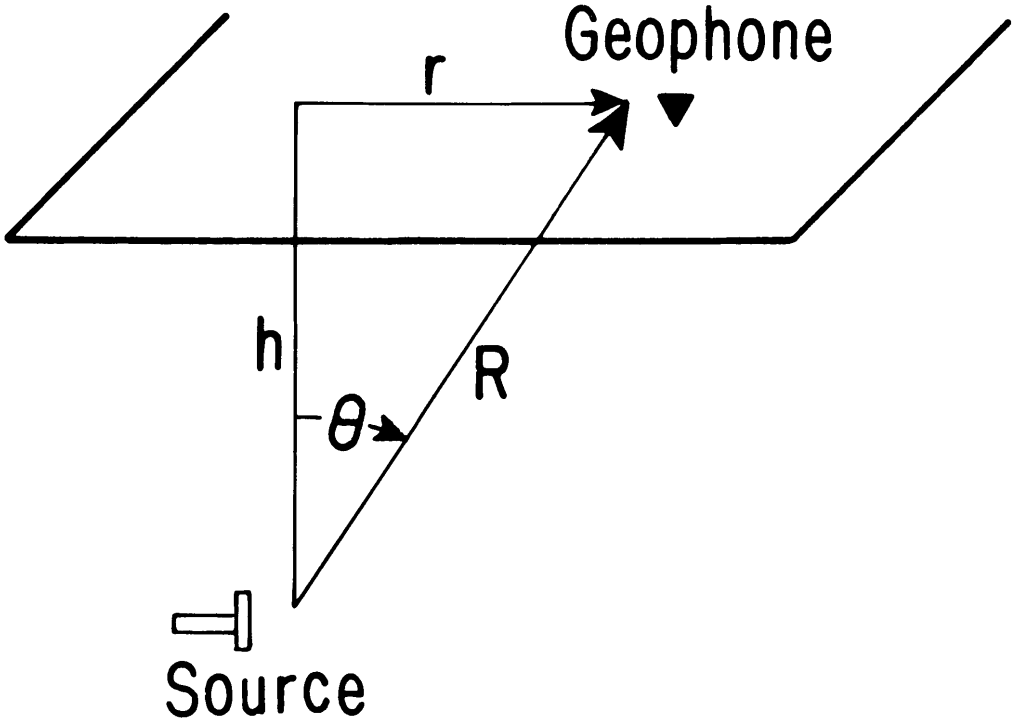

FIGURE 17. - Geometry for signal amplitude model and the form of model for earth velocity, V_e.

Each source, or large-timber blow on a roof bolt, is called an event, and for each event amplitudes were read on the seven subarrays. Six events for Peabody (h = 400 ft), 6 events for Hamilton #1, (h = 600 ft), and 12 events for Orient #6 (h = 800 ft) were used to fit for the average values of A_M, defined as $\tilde{A}_M$. The $\tilde{A}_M$ values were determined by first computing $\tilde{A}_{j,k,M}$ for k th subarray and j th event as

$$\tilde{A}_{j,k,M} = (\text{amplitude})_{j,k} \frac{R_{j,k}}{(\cos\Theta_{j,k})^M} . \qquad (7)$$

This then gave the $\tilde{A}_{j,k,M}$ for each of the three model forms for each measured amplitude. Then a least-squares criterion was used to determine the $\tilde{A}_M$ by minimizing the sum

$$S_M = \sum_j \sum_k (\tilde{A}_M - \tilde{A}_{j,k,M})^2 \ . \tag{8}$$

This criterion gives A_M as the mean of the $\tilde{A}_{j,k,M}$. A form of standard deviation (SD) was computed for the A_M by forming

$$SD_M = \sqrt{\frac{1}{N_s - 1}} S_M \ , \tag{9}$$

where N_s is the number of amplitude measurements in the sum. This procedure was done separately for the data at each mine and for the total data set from all three mines. The results are given in table 3.

TABLE 3. - Mean values for A_M and SD_M for the three Kentucky coal mines and for the total data set; μips-ft

Mine	A_1	SD_1	A_2	SD_2	A_3	SD_3
Orient #6	28,480	16,835	35,990	18,291	48,015	27,722
Hamilton #1	27,833	19,140	41,950	18,480	70,341	31,260
Peabody	26,597	14,757	35,266	18,657	48,204	26,465
Total data set	27,938	16,838	37,143	18,462	52,949	29,562
Cumulative probability for A:						
25 pct	34,000	NAp	46,000	NAp	65,000	NAp
50 pct (median)	23,000	NAp	34,000	NAp	76,000	NAp
75 pct	16,000	NAp	23,000	NAp	31,000	NAp

NAp Not applicable.

Table 3 shows that the values of each of the $\tilde{A}_M$ are fairly consistent between the three mines. The SD_M are approximately one-half to one-third the value of the corresponding $\tilde{A}_M$. This gives confidence in adopting a signal model that is characteristic of these three mines. The value used in the model was obtained using the whole data set. The M = 1 form was used since its total data set results provided the smallest ratio of $SD_M/\tilde{A}_M$.

Thus the model adopted for the average P-P amplitude of the earth velocity, V_e (h,r), for a large timber on a roof bolt is

$$V_e(h,r) = \frac{\tilde{A}_1 \cdot \cos \Theta}{R} \text{ (μips)} , \qquad (10)$$

where R is in feet and A_1 is the mean constant value for a large timber on a roof bolt, in microinches per second foot. A plot of the V_e (h,r) predicted by this model is shown in figure 18. To give an indication of how this model V_e (h,r) fits the data, data from the Hamilton No. 1 Mine (depth = 600 ft) are compared with V_e (600,r) in figure 19. The location of individual events is given by Westinghouse (25). The scatter of roughly 6 db observed on the plot is consistent with the SD of about 1/2 A_1.

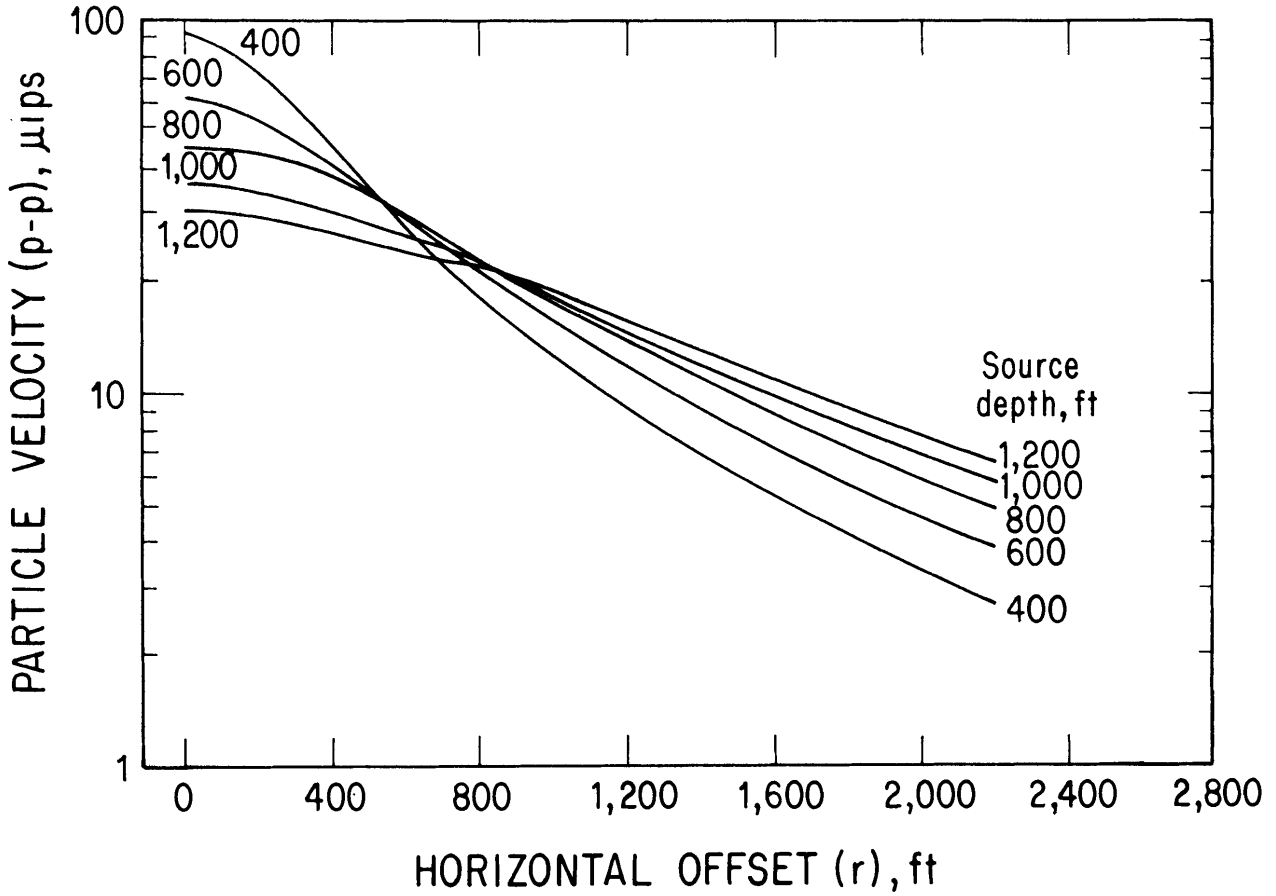

FIGURE 18. - Surface P-P particle velocity versus horizontal offset for A_1 model.

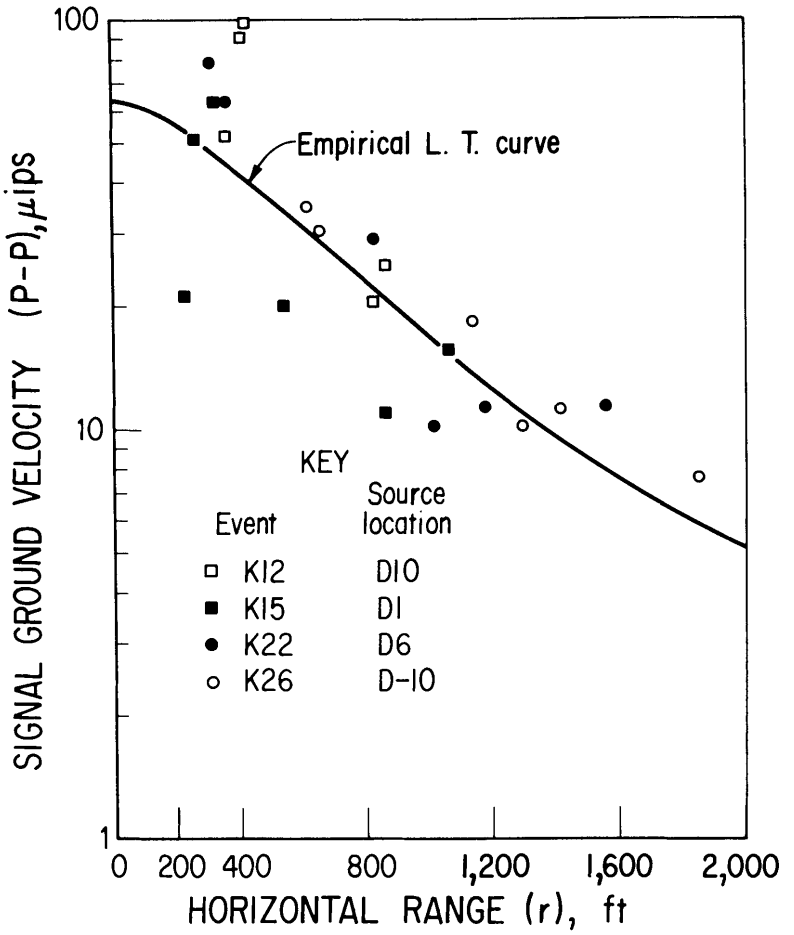

FIGURE 19. - Comparison of A_1 model predictions for signal amplitudes with Westinghouse data from the Hamilton #1 Mine.

As a further indication of the spread of the data values, cumulative probability curves have been plotted in figure 20, for $A_{j,k,M}$ with M = 1 and M = 2. Table 3 gives the 25 pct values (25 pct from largest), 50 pct values (median), and 75 pct values for $A_{j,k,M}$. In all cases the median values are close to the mean values. The 25-pct value is the signal amplitude that was exceeded 25 pct of the time; analogous definitions hold for the 50- and 75-pct values.

Signal Amplitudes From the 1977 Field Tests

In 1977, Westinghouse Electric Corp. carried out a series of seismic field tests at 12 mines (24). The primary purpose of these tests was to compile data from as many mines as possible to assess the ability of the seismic system to detect underground signals from trapped miners. Signals were observed at 11 of the 12 mines; signals were not observed at the Jim Walters #4 mine because the receivers had to be located in close proximity to various types of active machinery, and the high noise level caused by this machinery prevented detection.

The data from these tests were reduced by Westinghouse to give signal amplitudes for the sources that gave the largest values. For these field tests a large timber source gave the largest signal, and signal amplitudes were generally similar for application to the floor or to a roof bolt.

From the Westinghouse values of V_e, values of the constant A_1 were derived using the formula

$$A_1 = V_e \frac{R}{\cos \Theta} \qquad (11)$$

for each measured amplitude. For each mine all signals reported for a subarray location were averaged to give an average A_1 value for the location.

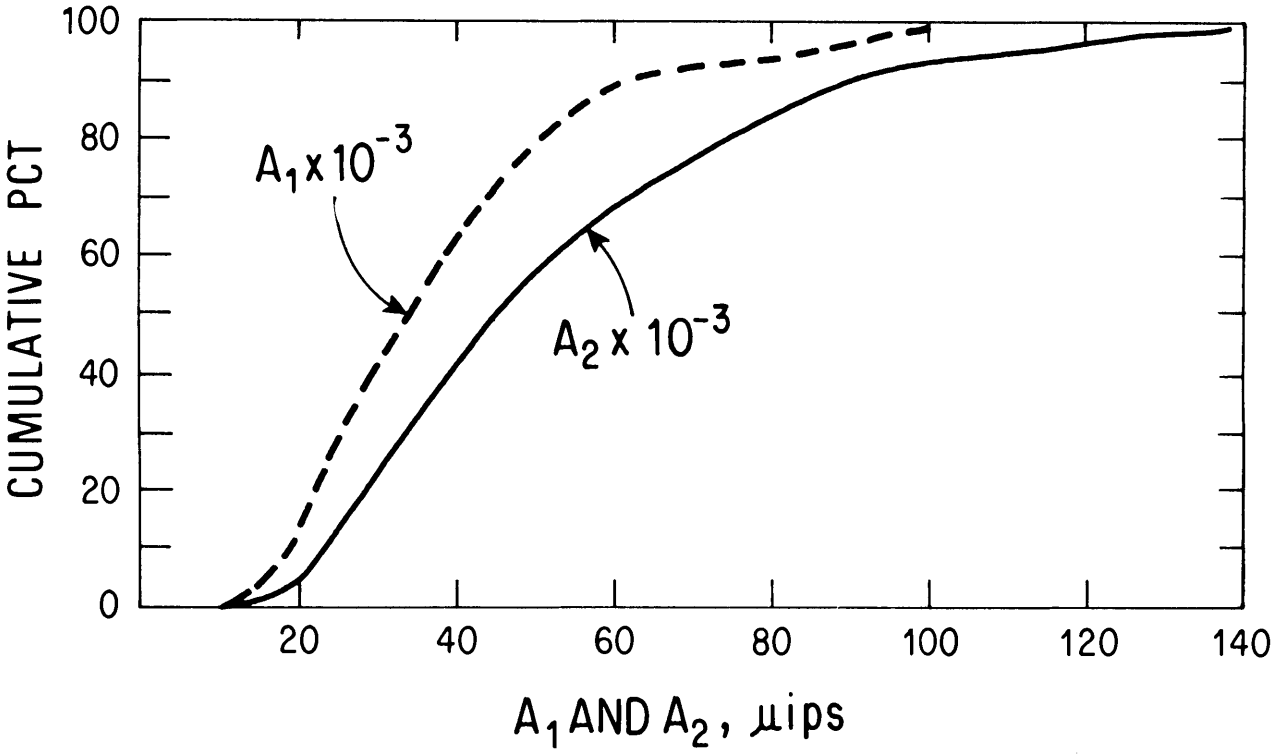

FIGURE 20. - Cumulative probability of A_1 coefficient and A_2 coefficient for three Kentucky mines.

Then the averages for each location were averaged to give an overall average value of A_1, called $\overline{A}_1$, for the mine; these values are given in table 4. The $\overline{A}_1$ values from these field tests were generally lower than those from the roof bolt blows of the 1976 Kentucky field tests; the difference may be due to calibration problems but could be due to soft roof conditions or to poor roof bolt coupling. Nevertheless, an overall average value for A_1 at the 14 mines is given in table 4.

TABLE 4. - Average value of A_1 for best source and noise amplitude and N and T values for Westinghouse 1977 data and 1976 Kentucky mine data

Mine	A_1 μips-ft (mine average)	Noise values (N), μips, (P-P)	$\overline{A}_1/N) = T$ (ft)
1977 tests:			
Mary Lee #1.....	9,800	3.4	2,882
Concord Mine.....	12,600	8.4	1,500
Jim Walters #3.....	14,300	6.0	2,383
Jim Walters #4.....	No data	No data	No data
Independent Salt Co.....	39,400	9.1	4,329
Bear.....	7,200	2.03	3,600
King.....	14,100	6.6	2,136
Starpoint.....	9,000	6.5	1,385
Staufer.....	13,000	2.3	5,652
Quarto #4.....	6,400	2.8	2,285
Hatters.....	3,400	2.2	1,545
VP #1.....	8,500	2.1	4,048
1976 tests:			
Orient #6.....	35,990	8.44	4,244
Hamilton #1.....	41,950	8.44	4,946
Peabody Camp No. 1.....	35,266	8.44	4,158
Average of 14 mines...	17,924	NAp	NAp

NAp Not applicable.

Also given in table 4 are the noise values, N, for the mines that were discussed in the first part of this section. From $\overline{A}_1$ and N values the ratio $T = \overline{A}_1/N$ was formed. This ratio is a distance-independent SNR which is critical to the ability of subarrays to detect the seismic signals. The significance of T is discussed in the section in "Detection Range."

The data from the 1977 tests were used to get a form of SNR and to examine the relative signal amplitudes from different source types. The 1977 data were not included in the calculations of the model for signal strength, which was completed before the 1977 tests. Also, there was some question about the gain of the amplifiers used in the seismic system during the 1977 tests, whereas for the 1976 tests, time was available to check the calibration by cross-checking several different seismic systems to assure accurate gains.

SIGNAL AMPLITUDE MODEL FOR VARIOUS SOURCES

In this section, signal models are developed which are applicable to sources other than the best-source type. This is done by relating the amplitudes from other source types to the amplitude from the best-source type. From the data an average difference in decibels between each of the source types and the best-source type is determined. This difference is called the adopted value.

In the majority of measurements the best signal was from a large timber applied to a roof bolt (denoted by source type, S1). There were exceptions to this; for example, it was noted (24) that at the Staufer Mine a large timber on the roof (there were no roof bolts) created weak signals because the roof was high, which made it difficult to use the large timber effectively. However, in general, the large timber on the roof bolt source amplitude was either the best source or within a few decibels of the best source. Thus, for the S1 source, a value of 0 db is adopted. This value is entered in table 5.

TABLE 5. - Signal amplitude of various sources relative to signal amplitude of a large timber on a roof

	Source S1	Source S2	Source S3	Source S4	Source S5	Source S6	Source S7	Source S8
Source type.....	Large timber.	Small timber.	Sledge	Large timber.	Small timber.	Hard hat.	Sledge	Rock pick.
Application point..	Roof bolt.	Roof bolt.	Roof bolt.	Floor	Floor	Roof bolt.	Floor	Roof bolt.
Orient #6 Mine..db..	NAp	-7	-8	-14	ND	-19	ND	ND
Peabody Mine...db..	NAp	-3	ND	-12	-16	ND	-14	ND
Peabody Mine...db..	NAp	-1	-3	ND	ND	ND	ND	ND
Concord Mine...db..	NAp	ND	-3	-4	-4	ND	ND	-7
Staufer Mine db.. (no roof bolts).	NAp	0	-1	+2	ND	-11	ND	ND
Value adopted db.. for C[1].	0	-3	-3	-8	-10	-15	-15	-7
A_1 (Sk)[2]..μips-ft..	[3]17,924	12,689	12,689	7,135	5,668	3,187	3,576	8,006

NAp Not applicable.
ND No data.
[1]Approximate average difference between amplitude from source type and amplitude from large timber hitting roof bolt.
[2]Obtained by reducing the value of $\overline{A}_1$ (S1) by the C value for each source.
[3]See table 4.

For other source types, representative differences between their amplitude and that from a large timber applied to a roof bolt are given. From these data approximate average differences, C, are formed; these C values are rough estimates of the difference in signal amplitude between the best source and others.

Based on C values for the source types S2 to S8, an estimate was made of the $\overline{A}_1$ (Sk) constant for each source type. This was obtained by reducing the value of $\overline{A}_1$(S1) = 17,924 μips-ft from table 5 by the C value for each source. With the Al (Sk) values of table 5 the signal amplitude model for each source type is given by

$$V_e\ (Sk) = \frac{\overline{A}_1(Sk)\ \cos\ \Theta}{R}\ . \qquad (12)$$

DETECTION CRITERION

In this section the criterion for signal detection is developed. The criterion that will be used in this report is that the P-P signal amplitude be greater than the P-P noise envelope.

A reasonable approach is to consider that a threshold is set which will be exceeded by the noise once in 100 sec. The normal bandwidth of the system is 180 Hz; however, as discussed in the section on seismic noise, the power is concentrated in roughly the lower half of this frequency range. Thus, it is reasonable to use an equivalent bandwidth of 25 Hz in computing the time between independent samples of noise amplitude. Thus in 100 sec, 7,500 independent values of the envelope occur. In the appendix it is shown that if the zero-to-peak threshold R_o is set to 4.22 σ_N, the envelope will have a probability of exceeding the threshold of 1/7500, thus giving the desired false alarm rate of once every 100 sec. Here σ_N is the the rms noise value.

Therefore a 4.22 σ_n zero-to-peak threshold or a 8.44 σ_n P-P threshold will be used. It will be assumed in this report that a signal will be detected if its P-P amplitude is above this value.

It is noted that the assumptions that a signal whose amplitude is above the threshold will always be detected and that a signal whose amplitude is below the threshold will never be detected are not strictly valid. However, detection done manually or by an automatic computer algorithm is a complex process. Therefore, it is not felt that a more complex criterion than the one adopted is presently justified. Digital analysis of an extensive data set in the future could justify a more complex criterion.

DETECTION RANGE

The range at which a single geophone or subarray can detect a source depends on the signal amplitude and the noise level. In this section universal curves are given that allow an estimation of the maximum horizontal range at which a signal of a given strength can be detected under a known noise condition. The M = 1 signal model is used. Let A_1 be the constant for the source under consideration. On the basis of the M = 1 signal model the condition for detection is that

$$\frac{A_1}{R} \cos \Theta > N \ . \tag{13}$$

Define the quantity $T = A_1/N$. Then T is a measure of the size of the generated signal divided by the noise and is independent of the source depth h and the horizontal offset between the source and geophone. In table 6, values of T are given for large timber sources. These values, which are the individual mine averages, range from 1,500 to 5,652 ft. For other source types, the T values are adjusted by the factors given in table 6. Using the range of 1,500 to 5,652 for the large timber on the roof bolt source and the table 5 adopted

value adjustments, the range of T values expected for various sources is compiled in table 6.

TABLE 6. - Range of T values for various sources

	Feet
Large timber on roof bolt.....	1,500-5,652
Small timber on roof bolt.....	1,062-4,001
Sledge on roof bolt.....	1,062-4,001
Large timber on floor.....	597-2,250
Small timber on floor.....	474-1,787
Hard hat on roof bolt.....	267-1,005
Sledge on floor.....	299-1,128
Geopick on roof bolt.....	670-2,525

Then the condition for detection can be written

$$T = A_1/N \geq R/\cos \Theta \ . \qquad (14)$$

Based on this criterion, curves were calculated (fig. 21) that give the maximum horizontal range for detection, r_m, as a function of the source depth, h. Note that the maximum value of r_m for a given T does not occur for a very shallow source. Rather it occurs for the value of h which is half the mixiumum h at which a source can be detected. For example, if T = 1,500 ft, the maximum depth at which a source is detectable is 1,500 ft and the maximum of r_m occurs at h = 750 ft. The reason that the greatest r_m does not occur for the most shallow sources is that the radiation pattern is such that the outgoing signal has a cos Θ = h/r dependence; therefore, when h/r is small, the signal is small.

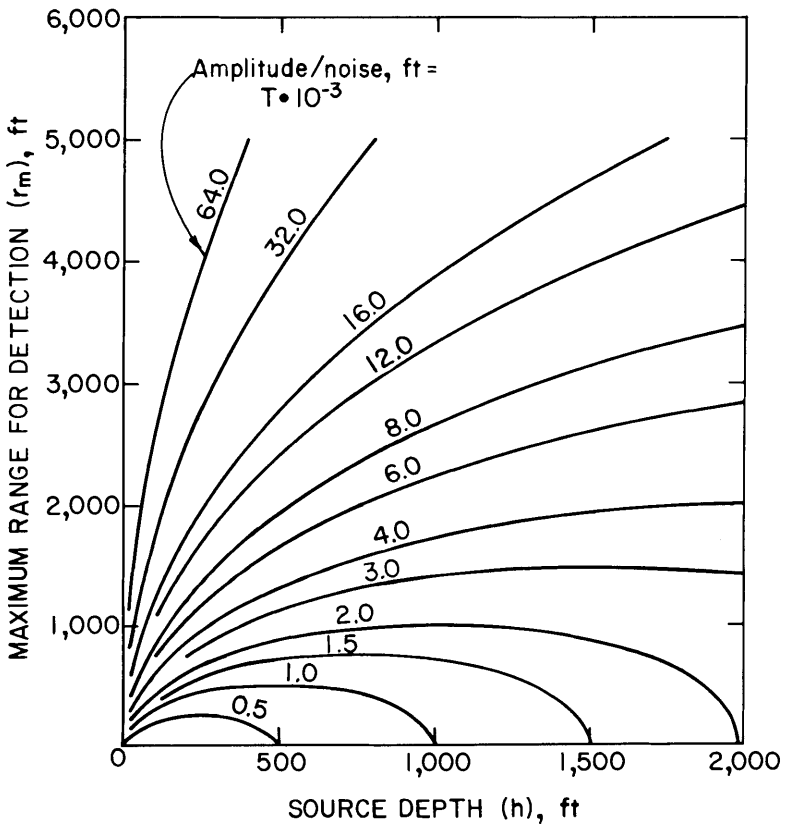

FIGURE 21. - Maximum horizontal detection range versus source depth.

SUBARRAY PERFORMANCE

The seismic rescue system uses an array composed of seven subarrays rather than seven individual geophones to receive seismic signals because a subarray will give a better SNR than the single geophone. This

improvement is achieved principally in three ways. First, noise that is uncorrelated between the geophones will be reduced in amplitude by $\sqrt{N}$ by the cancellation that occurs by averaging zero mean random numbers. Second, noise that is propagating at a slow horizontal velocity will be reduced on the output of the subarray because, if the subarray is thought of as an antenna, the noise will be outside of the antenna's main beam. Finally, any adverse effects that would result if a single badly planted geophone were used will be alleviated by the averaging of all the subarray geophone outputs.

A subarray output Y(t) is formed by averaging the individual geophone inputs, $X_i(t)$, as

$$Y(t) = \frac{1}{N} \sum_{i=1}^{N} X_i(t) \quad . \tag{15}$$

Thus, the formation of the subarray output can be thought of as forming an averaging of the individual inputs. $X_i(t)$ is composed of two parts: $N_i(t)$, the noise; and $S_i(t)$, the signal from the trapped miner. In this section the SNR gain will give the improvement of a subarray compared to the single geophone. In determining this, both the noise reduction by the subarray and the effect of the subarray on the signal amplitude will be considered.

As mentioned before, two subarray configurations have been developed and used extensively. The first is a seven-geophone subarray Westinghouse (24) with a 4.5-m diameter having the geophones wired in parallel. The second is a larger 24-geophone subarray with a 24-m diameter. This large subarray uses two series-connected strings of 12 geophones with the 2 strings connected in parallel (6). The subarrays are shown in figure 3. The electronic configurations of both subarrays are such that the sensitivity of the subarrays is well below even low levels of natural seismic noise. Thus, the ability to detect and identify signals from an underground miner is determined by the seismic noise level.

The use of a subarray will normally result in some loss of amplitude compared with using a single geophone, in measuring a signal from a miner hitting below ground. This signal loss is due to the fact that the signal is not exactly the same on each subarray geophone. For a miner directly below the subarray the signal is in phase at all geophones and the signal loss will be minimal. However, for sources horizontally offset from the subarray there is a phase shift (or equivalently an arrival time difference) between the geophones.

The signal output of the subarray is

$$S_o = \frac{1}{N} \sum_{i=1}^{N} S_i \quad . \tag{16}$$

Let the N elements of the subarray be located at the points $\vec{r}_i$ on the earth's surface. The signal is of the form $e^{i(\omega t - \vec{r}_i \cdot \vec{k})}$ where $\vec{k}$ is the wavenumber vector. Note $|\vec{k}| = \omega/V_H$, where $V_H = (V/\sin \Theta)$ is the horizontal phase velocity of the wave. Here V is the wave velocity and Θ, the angle of incidence, is the angle the ray makes with the vertical. The geometry of this situation is shown in figure 17. When the magnitudes of the signals are equal on all seismometers, the signal output compared to a single geophone is (in db)

$$G_s = 20 \log \left| \frac{1}{N} \sum_{i-1}^{N} e^{-i(\vec{r}_i \cdot \vec{k})} \right|. \qquad (17)$$

For a signal that is identical and in phase at all geophones (this requires $V_H = \infty$, so $\vec{k} = 0$), $G_s = 0$ db. This would approximately be the case for the small seven-geophone subarray where signal loss is not significant. The 24-geophone subarray was designed to be as large as possible without causing unacceptable signal loss. For the 24-geophone subarray the loss at frequencies below 50 Hz is negligible. For 100 Hz and angles Θ of greater than 35°, signal losses are in excess of 3 db compared with a single geophone. However, field test results discussed by Durkin and Greenfield (6) indicated that very rarely were signal losses above 1 or 2 db for the 24-geophone subarray. One reason that signal amplitude decreases of more than 3 db were rare with the 24-element subarray is that for Θ's greater than 30° or 40° the signals usually do not have a major portion of their power above 60 or 70 Hz. Thus, signal amplitude loss due to the subarray does not appear to be a serious problem.

The noise reduction for noise that is incoherent between the geophones is 20 log N (db). This is a gain of 13.8 db for the 24-geophone subarray and 8.5 db for the 7-geophone subarray. Seismic noise that is completely incoherent is not the normal situation but occurs during rain. In this situation the noise level is high and thus the subarray gain is especially important. Field test results have verified that this gain occurs during rain. In areas with brush or high grass ground cover the noise generated by the wind may also be essentially incoherent between geophones. The larger spacing between geophones of the 24-geophone subarray compared with the 7-geophone subarray enhances the possibility that the noise will be incoherent.

In many situations the seismic noise may be highly coherent between the subarray geophones; however, the subarray can still give noise reduction because the noise is not in phase between the geophone (3).

The source of coherent noise may be wind acting on trees outside of the subarray, distant traffic, machinery, or airborne noise. Much seismic noise at frequencies of 20 to 200 Hz is of low horizontal phase velocity, V_H, since it travels at an acoustic velocity (330 m/sec) or at seismic surface wave velocities, which are usually below 1,000 msec.

In practice there could exist many surface noise sources propagating with different V_H and at different angles of incidence on the subarrays (17). It is instructive to study the expected attenuation of these waves by the subarrays by choosing waves of discrete frequency and velocity within the ranges of interest and treating the angle of incidence of the waves on the subarray as a random variable.

The output of a subarray for a horizontally traveling wave is

$$Y = \frac{1}{N} \sum_{i=1}^{N} e^{(\vec{k}_N \cdot \vec{r}_i)} \tag{18}$$

where Y is the normalized amplitude of the noise output and $\vec{k}_N$ is the horizontal wavenumber of the noise.

The noise reduction is G = 20 log Y db.

Table 7 gives an indication of the subarray noise rejection for the 24-element and 7-element subarrays, as a function of frequency and V_H. The horizontal phase velocity of the wave is related to the wavenumber by $V_H = \omega/k_N$. The noise reduction depends on the direction as well as V_H. The values in these tables are the smallest noise reductions (worst case) for any direction. These tables were constructed from more extensive tables generated by a computer program based on equation 18.

TABLE 7. - Theoretical subarray noise reduction, db

(Minimum in any direction)

V_H, m/sec	Frequency					
	15 Hz	30 Hz	45 Hz	60 Hz	90 Hz	120 Hz
24-ELEMENT SUBARRAY						
200.....	14.0	7.6	9.2	11.0	7.2	7.7
300.....	17.0	15.0	7.6	13.0	11.0	15.0
330.....	25.0	18.0	6.2	13.0	10.0	9.5
400.....	17.0	14.0	11.0	7.6	9.2	11.0
600.....	5.6	17.0	14.0	15.0	7.6	14.0
800.....	2.9	17.0	14.0	14.0	11.0	7.6
1,000.....	1.8	9.7	27.0	13.0	18.0	8.8
1,500.....	.8	3.4	8.7	22.0	13.0	16.0
7-ELEMENT SUBARRAY						
200.....	2.7	11.0	15.0	10.0	1.2	3.8
300.....	1.0	4.2	11.0	25.0	10.0	4.8
330.....	.8	3.4	8.9	24.0	11.0	9.8
400.....	.5	2.3	5.6	12.0	16.0	10.0
600.....	.2	1.0	2.3	4.2	12.0	25.0
800.....	.1	.5	1.3	2.3	5.6	12.0
1,000.....	.1	.3	.8	1.4	3.4	6.5
1,500.....	.0	.1	.3	.6	1.4	2.6

The 24-element subarray will suppress most coherent low V_H noise for frequencies of 30 Hz and larger quite well. The worst case noise reduction values for coherent noise are generally nearly as large as the incoherent noise reduction. Note that the subarray reduction of coherent noise can be above or below the reduction of incoherent noise.

The seven-element subarray does well against coherent noise at horizontal wavelengths, V_H/f, below approximately 10 m. For the higher velocities and/or lower frequencies, the seven-element subarray does not give significant noise reduction.

From the above theoretical considerations of SNR improvement by the 24- and 7-geophone subarrays, it is to be expected that the 24-geophone subarray would offer a significant SNR gain over the 7-geophone subarray. In an extensive series of field tests this was often the case (6). Typical gains were 5 db for the 7-geophone subarray and 10 db for the 24-geophone subarray. There were, however, some mines where the SNR of the two subarray types were comparable. The 7-geophone subarray, however, may offer practical advantages in terms of deployment where a clear area cannot be found to deploy the larger 24-geophone subarray.

PROBABILITY OF DETECTION

It is desirable to determine the probability that a given surface array will detect an underground source. In the configuration normally used, seven

subarrays are placed on the surface to monitor a portion of the subsurface. A method has been developed to calculate the probability that m subarrays or more, with $1 \leq m \leq 7$, will detect a miner's signal. The detection of a signal by one subarray may be sufficient to identify the signal as coming from an underground miner. However, identification can be more certain if several subarrays can detect the signal. To locate, at least three subarray detections are required, and five or more are desirable for accurate location.

Figure 22 shows a surface array monitoring a volume of the subsurface. The criterion for detecting a signal from a given underground location with subarray k is

$$T > \frac{R_k}{\cos \theta_k} . \qquad (19)$$

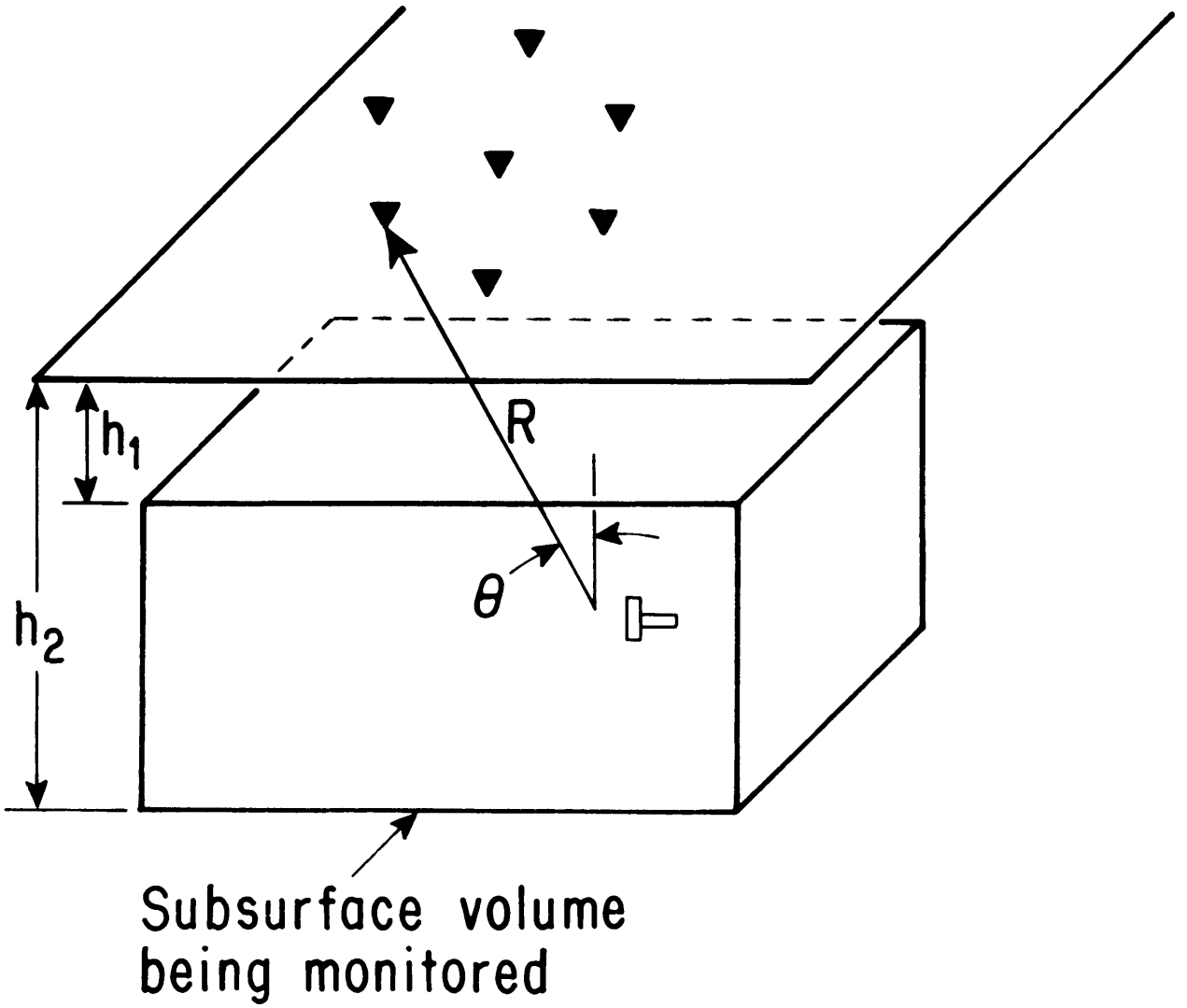

FIGURE 22. - Geometry for calculation of detection probability. Triangles indicate subarray locations.

If T is treated as a random variable, then the probability of detecting with subarray k is the probability that $T > \frac{R_k}{\cos \theta_k}$. To apply this detection criterion the probability destribution was developed using the best source (large timber) type values for T given in table 4. The 14 values were ordered and plotted as a cumulative distribution in figure 23. For convenience this observed distribution was fit with the chi-square cumulative probability function (1), $P(X^2|\delta)$. It was found that using the number of degrees of freedom, $\delta = 6$, and $X^2 = T/550$ gave a good fit to the data. In other words, the fit chi-square curve, shown in figure 23, states that the probability that $T \leq T_o$ is given by

$$P\left(\frac{T}{550}\,\middle|\,6\right) = \frac{1}{2^3 2!}\int_0^{To/550} t^2 e^{-3}dt \ . \qquad (20)$$

The notation $P_L(To)$ will be used for $P\left(\frac{T}{550}\,\middle|\,6\right)$, the cumulative distribution of T, and notation $Q_L(To) = 1 - P_L(To)$ will be used as the probability that T exceeds To. The probability of detection with a large timber source is then given by $Q_L\left(\frac{R_k}{\cos \theta_k}\right)$. Note that the T data used were average values for

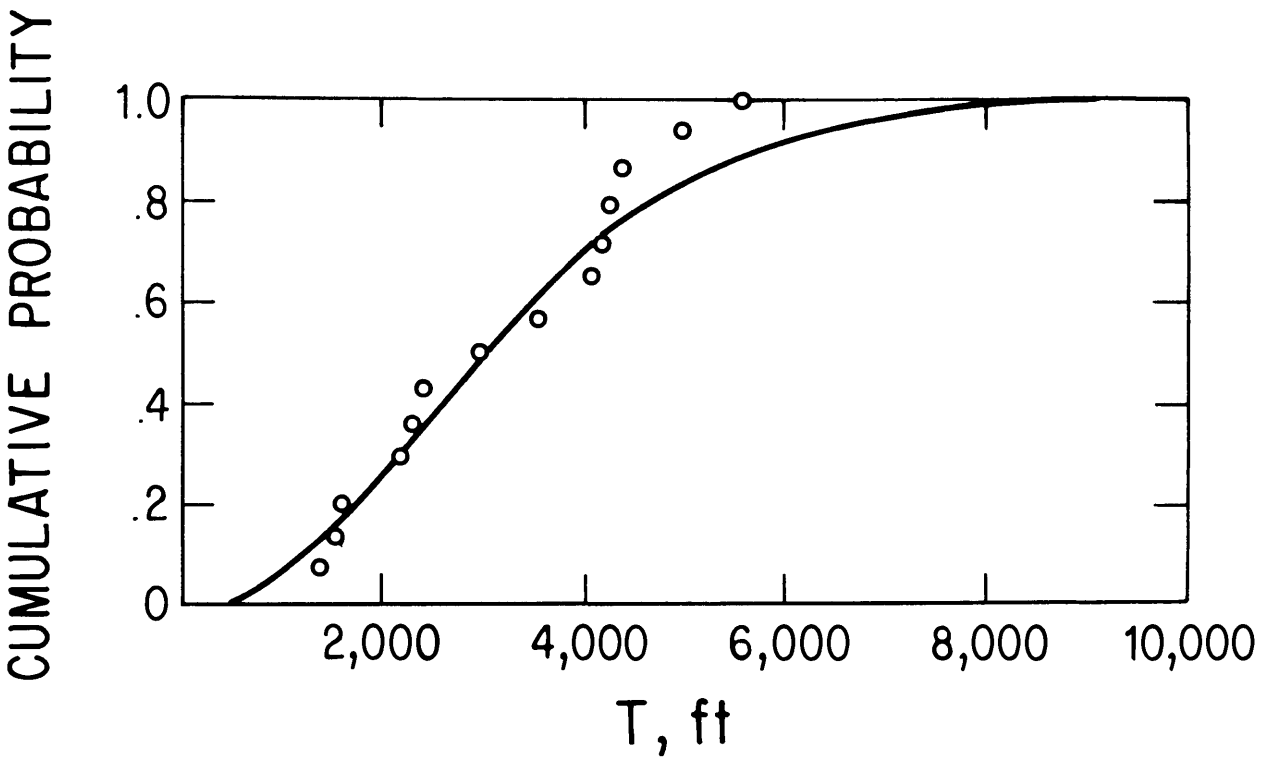

FIGURE 23. - Chi-square fit to cumulative probability of T.

individual mines. If the individually measured T values were to be plotted as a cumulative distribution, the curve could be expected to be similar to the mine averages.

For a source other than the large timber on a roof bolt, reasonable cumulative probability curves for T can be estimated by using Q (To · C) for the curve. Here C is the factor, which is given in db in table 8, that gives the amplitude of a particular source type relative to the large timber source S1.

Let $Q_L\left(\frac{R_k}{\cos \Theta}\right)$ where k = 1,2,...,7 be the probability that the k subarray will detect the signal from a source at r_k. Next calculate the probability of m and only m subarrays detecting the signal (8, pp. 89-96):

$$P_{[m]}(r_i) = S_m - \binom{m+1}{m} S_{m+1} \tag{21}$$

where $\binom{m+1}{m}$ are the binomial coefficients,

$$S_1 = \Sigma P_i,\ S_2 = \Sigma P_{i,j},\ S_3 = \Sigma P_{i,j,k},\ \text{etc.} \tag{22}$$

Here $P_i = Q_L\left(\frac{R_i}{\cos \Theta_i}\right)$ $P_{i,j} = Q_L\left(\frac{R_i}{\cos \Theta_i}\right) \cdot Q_L\left(\frac{R_j}{\cos \Theta_j}\right)$ (23)

and $P_{i,j,k} = Q_L\left(\frac{R_i}{\cos \Theta_i}\right) \cdot Q_L\left(\frac{R_j}{\cos \Theta_j}\right) \cdot Q_L\left(\frac{R_k}{\cos \Theta_k}\right)$. (24)

The sums in the definition of the S are taken such that if $i<j<k<\cdots 7$, then each combination appears once and only once in the sum. The probability of m or more subarrays detecting the signal is denoted by $P_m(r_i)$ and is given by

$$P_m(r_i) = \sum_{k=m}^{7} P_{[k]}(r_i) . \tag{25}$$

First it is necessary to obtain the average value of P_m for detecting the signal from a source which is at some depth h but which can be located with equal probability in some horizontal region of the mine. This probability of detecting with m or more subarrays is denoted by $\hat{P}_m$ (h) and is given by

$$\hat{P}_m(h) = \frac{1}{A(h)} \int_A P_m(r_i)\, dx\, dy . \tag{26}$$

Here A(h) is the area of the mine at depth (h). To get the overall average probability $\hat{\hat{P}}_m$ of detecting with m or more subarrays for a source in the volume shown in figure 22, which extends from h_1 to h_2, use

$$\hat{\hat{P}}_m = \frac{1}{h_2 - h_1} \int_{h_1}^{h_2} \hat{P}_m(h)\, dh \tag{27}$$

$$\hat{\hat{P}}_m = \frac{1}{VOL} \int_{h_1}^{h} dh \int_{A} P_m(h)\, dx\, dy \; . \tag{28}$$

To evaluate $\hat{P}_m$ and $\hat{\hat{P}}_m$ the integrals are approximated by sums over a three-dimensional grid covering the volume of interest.

In the following three examples the volume considered was a right-rectangular prism with top at h_1 = 200 ft and bottom at h_2 = 1,200 ft. This depth range is consistent with the fact that the majority of mines lie in this range.

Figure 24 is the first example of the results of the calculations. The plan view shows an array of seven subarrays with a 500-ft radius. The subsurface being monitored is a square having sides of 2,000 ft. For the large timber on a roof bolt source with no subarray SNR improvement, one looks at the 0-db position on the abscissa to get the probability of m or more subarrays detecting. For example, the probability of m = 5 or more detecting is 0.62 (index base 1.00). From table 5 the signal for a small timber on a roof bolt (S2) has C = -3 db. Thus, one looks at the -3 db abscissa value for an S2 source. Note that for any source type the use of the subarrays gives approximately a +5-db improvement in SNR compared with the single sensor values. After a single subarray has detected a signal, the stacking of successive blows will also improve the SNR. If 10 blows are stacked a 10 db improvement is commonly obtained. Thus, for the case of locating the source using stacked traces from the subarrays, the C = +15 db value applies for the large timber on the roof bolt.

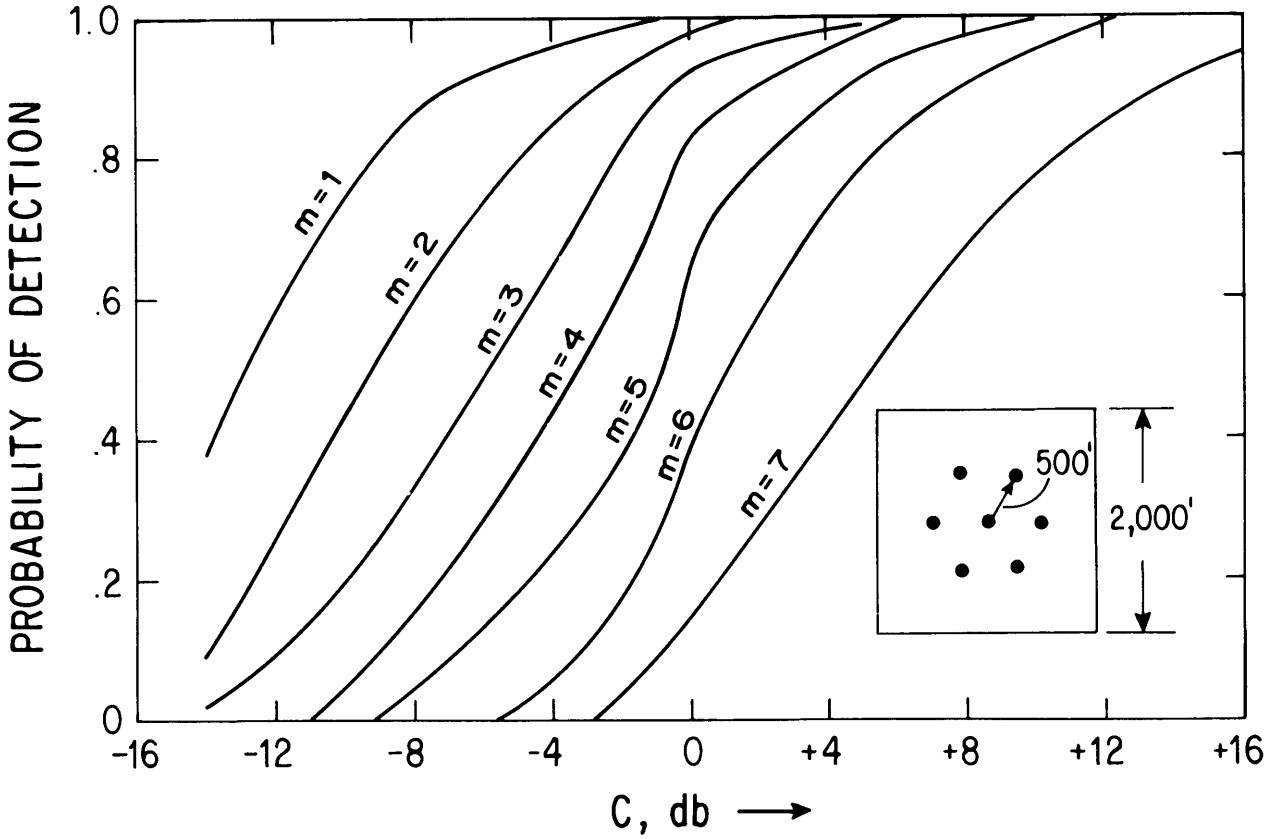

FIGURE 24. - Probability of detection by m or more subarrays versus C, the ratio of T to the large timber T–500-ft array radius, 2,000-ft monitored square.

Thus for large timber sources for the figure 24 configuration it is very likely that at least one subarray will initially detect the signal; after stacking, signals should be seen on the five or more subarrays that are desirable for accurate location.

Figures 25 and 26 show corresponding results for the monitoring of a square having sides of 4,000 ft for array radii of 500 ft and 1,000 ft. Since a large area is being monitored, the detection probabilities are lower than for the 2,000-ft square.

For the monitoring of the 4,000-ft square with an array centered at the center of the square, the effect on the detection probability of the array radius was examined. This was done for the value C = 0 db; that is, for the best source with no array gain or stacking. Results are shown in figure 27. To obtain a signal from at least one subarray, the use of the larger radius arrays is somewhat better. The reason for this is that for the 500-ft-radius-array points on the boundary of the square will be a minimum of 1,500 ft horizontally removed from the nearest subarray. Thus, to have the maximum probability of detection, it is suggested that before a signal is found it might be best to use a 1,000-ft-radius array when monitoring such a large area. If conditions allow, after detection on a single subarray, it would

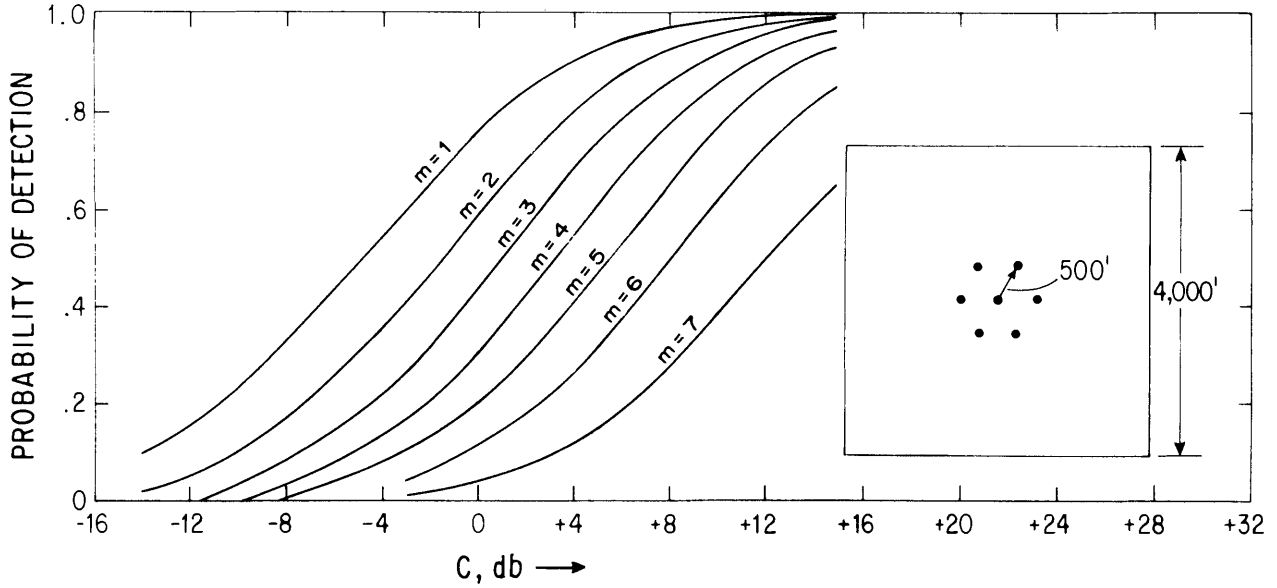

FIGURE 25. - Probability of detection by m or more subarrays versus C, the ratio of T to the large timber T–500-ft array radius, 4,000-ft monitored square.

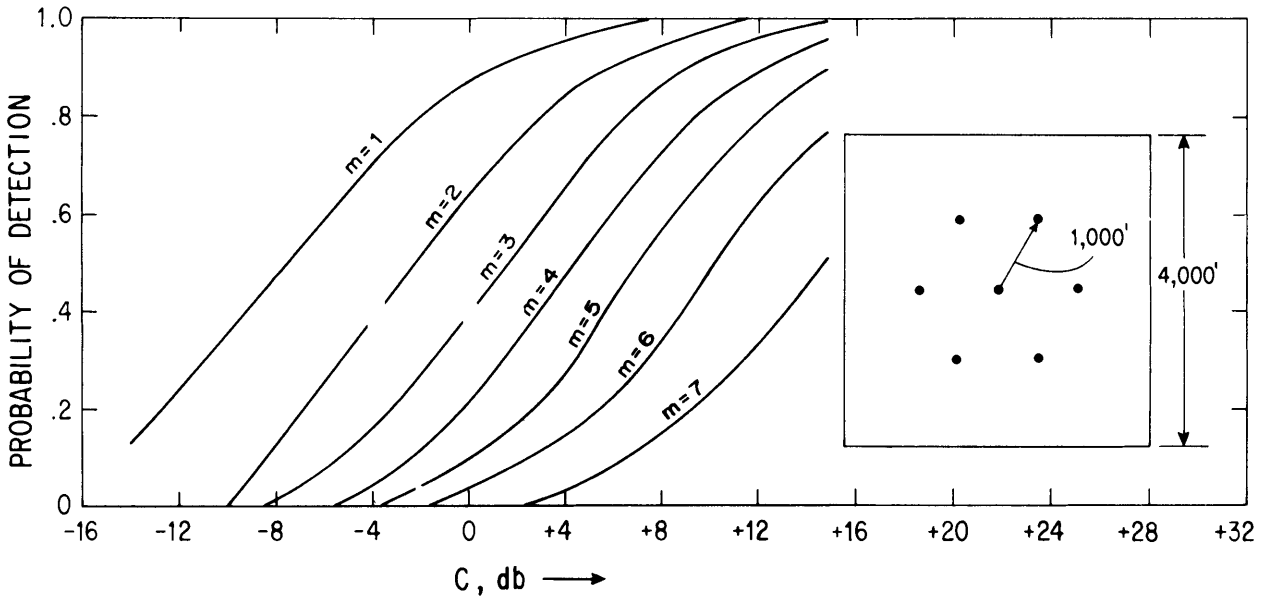

FIGURE 26. - Probability of detection by m or more subarrays versus C, the ratio of T to the large timber T–1,000-ft array radius, 4,000-ft monitored square.

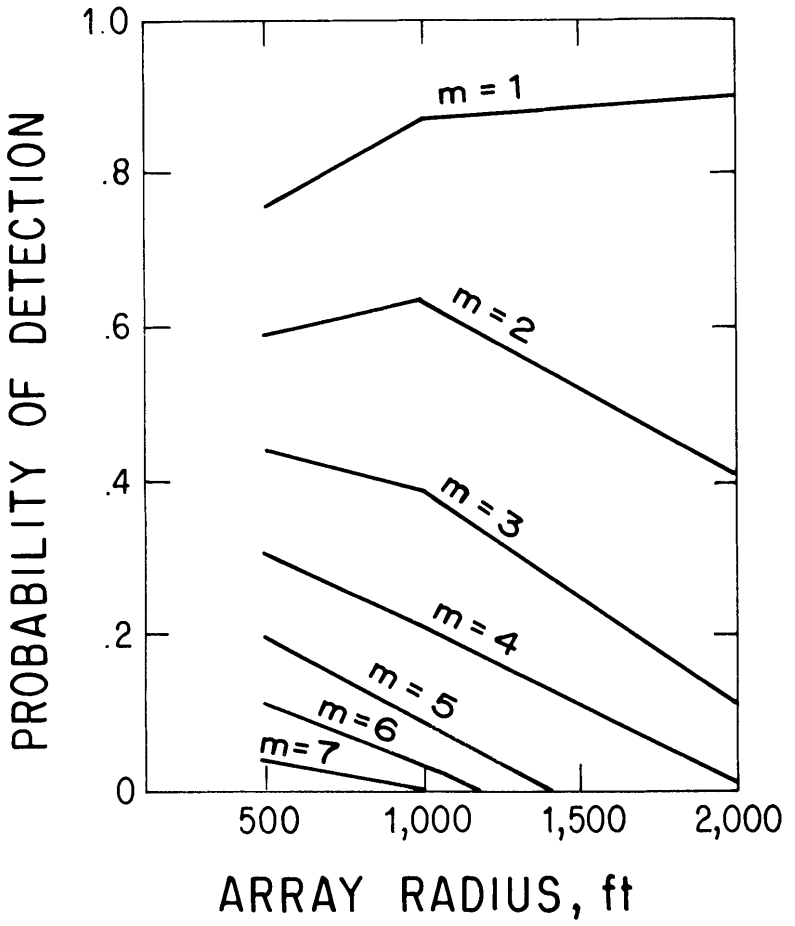

FIGURE 27. - Probability of detection with m or more subarrays versus array radius, large timber source (C = 0 db), 4,000-ft monitored square.

then be desirable to move some of the distant subarrays to the vicinity of the detecting subarray and signal the trapped miner to repeat his signal to allow improved location.

Next the situation will be examined where the trapped miner is believed to be below a particular point. One subarray would be set directly above that point. The probability of detecting that miner can be calculated by fixing the subsurface region to be monitored as a very small area directly below the central subarray of a 1,000-ft-radius array. Calculations were made, and results are shown in table 8. For a source 500 ft deep even a weak source with C = -10 db will be detected with 0.85 probability. Noting that a 24-geophone subarray gives a 5- to 10-db SNR improvement, it is expected that a subarray would probably detect the signal even for sources down to 2,000 ft. This high probability of seeing a source directly below a subarray is consistent with the fact that in field tests signals from sources directly below a subarray were consistently detected.

TABLE 8. - Probability of detection for a subarray directly above the source

Depth, ft	Amplitude of particular source type relative to large timber source (C)					
	-15 db	-10 db	-8 db	-5 db	0 db	+5 db
500.....	0.53	0.85	0.93	0.99	1.00	1.00
1,000.....	.13	.65	.87	.99	1.00	1.00
1,500.....	.02	.42	.72	.96	1.00	1.00
2,000.....	.00	.21	.49	.87	1.00	1.00
2,500.....	.00	.09	.28	.72	.99	1.00

For convenience in considering the probability of detecting a source under various situations, table 9 was compiled. For this table it was assumed that the postdetection stacking would give a 10-db SNR improvement, which is what has been observed. Also, a 5-db gain for subarray use has been included for two of the five sources. The table gives the probability of detecting with one or more and with five or more subarrays. The one or more case is most important in the detection process, and five or more case in the location process.

TABLE 9. - Probability of detection with one or more and with five or more subarrays

Source type	Assumed subarray gain, db	Mine area 2,000 by 2,000 ft, 500-ft array radius			Mine area 4,000 by 4,000 ft, 1,000-ft array radius		
		1 or more	5 or more	5 or more with stacking	1 or more	5 or more	5 or more with stacking
Large timber (with gain).....	+5	1.00	0.92	1.00	0.96	0.35	0.90
Large timber.....	+0	1.00	.64	.99	.87	.09	.68
Sledge on roof.....	+0	.99	.37	.98	.80	.05	.56
Rock pick on roof.....	+5	.97	.30	.96	.78	.02	.50
Sledge on floor.....	+0	.38	.00	.25	.13	.00	.00

It is instructive to observe the variation in the probability of detection as depth is varied. These results are shown in figures 28-31. The probability of detecting a miner's signal was determined when using an array of a 1,000-ft radius over square areas of 0.5 and 1.0 mile on a side, for varying depth. Probabilities were determined for weak and strong sources with and without processing. This processing takes the form of stacking. Also considered was whether detection is probable on one or more subarrays ($m \geq 1$) or five or more subarrays ($m \geq 5$).

The detection probabilities discussed have all been based on the use of subarrays made of geophones that measure the vertical particle velocity of the ground. Geophones that measure the horizontal particle velocity are also manufactured and have been used in a limited number of experiments. The results of these experiments indicate that most often the vertical geophones outperform the horizontal geophones. There have been exceptions to this; the cases where horizontal geophones gave better performance have occurred where the angle θ (see fig. 17) is fairly large. This result is consistent with the radiation patterns of P- and S-type seismic waves. Often in these situations it is the S wave on the horizontal that is the largest signal. To employ horizontal geophones two extra channels (one for north-south and one for east-west polarization) at each subarray location must be employed. When using horizontal geophones each geophone must be carefully oriented. The signals from horizontal phones are often more difficult to interpret. Therefore, the logistics of the operations suggest that for the surface seismic location system the present vertical geophone system should be maintained, rather than a mixed vertical and horizontal system.

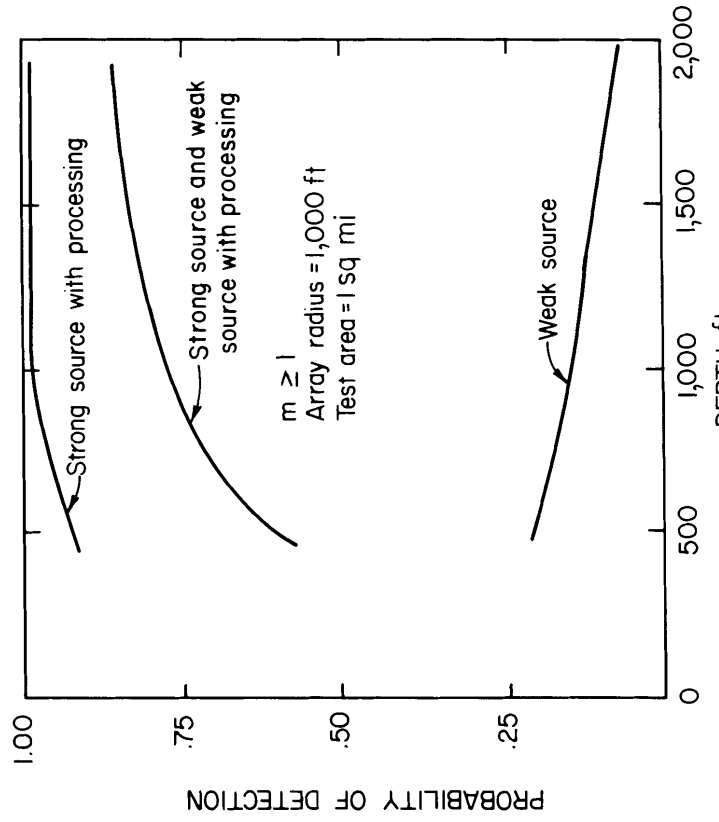

FIGURE 29. - Probability of detecting a miner's signal as a function of depth by one or more subarrays in an array of 1,000-ft radius monitoring a square area 1.0 mile on a side.

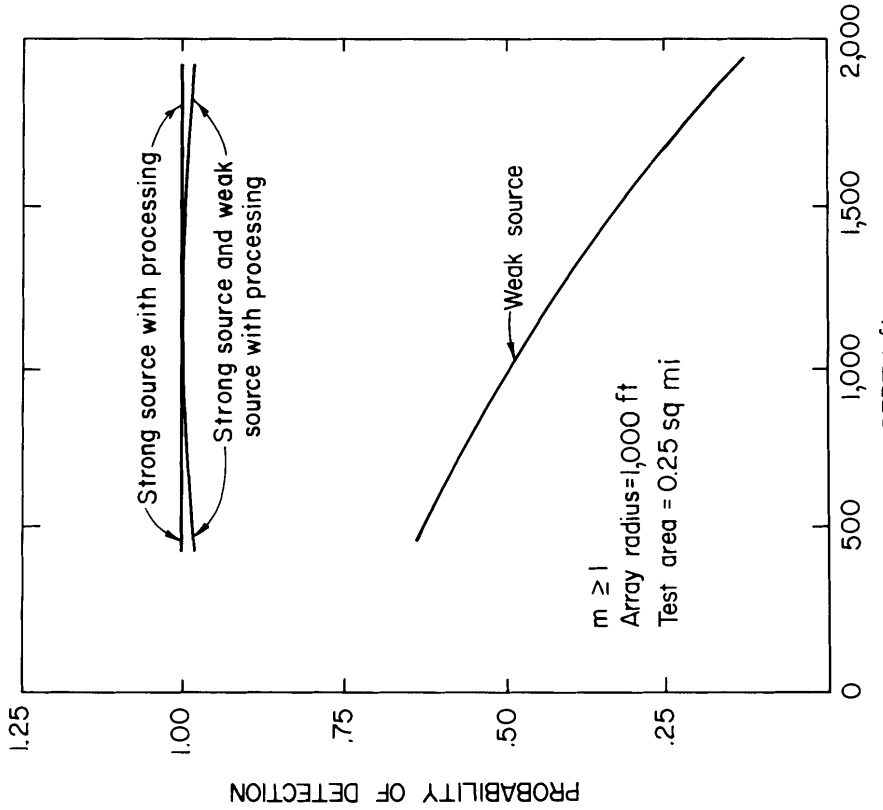

FIGURE 28. - Probability of detecting a miner's signal as a function of depth by one or more subarrays in an array of 1,000-ft radius monitoring a square area 0.5 mile on a side.

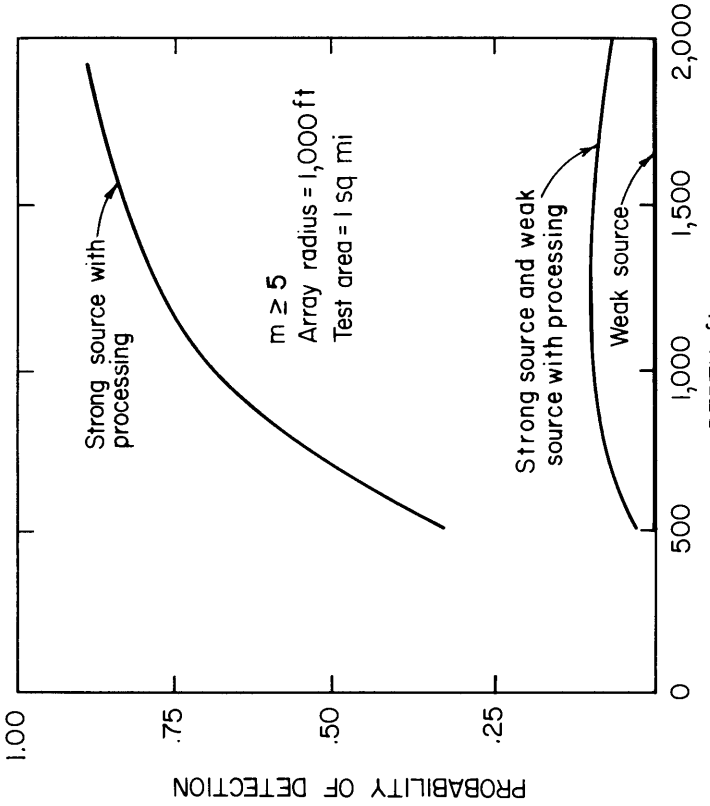

FIGURE 31. - Probability of detecting a miner's signal as a function of depth by five or more subarrays in an array of 1,000-ft radius monitoring a square area 1.0 mile on a side.

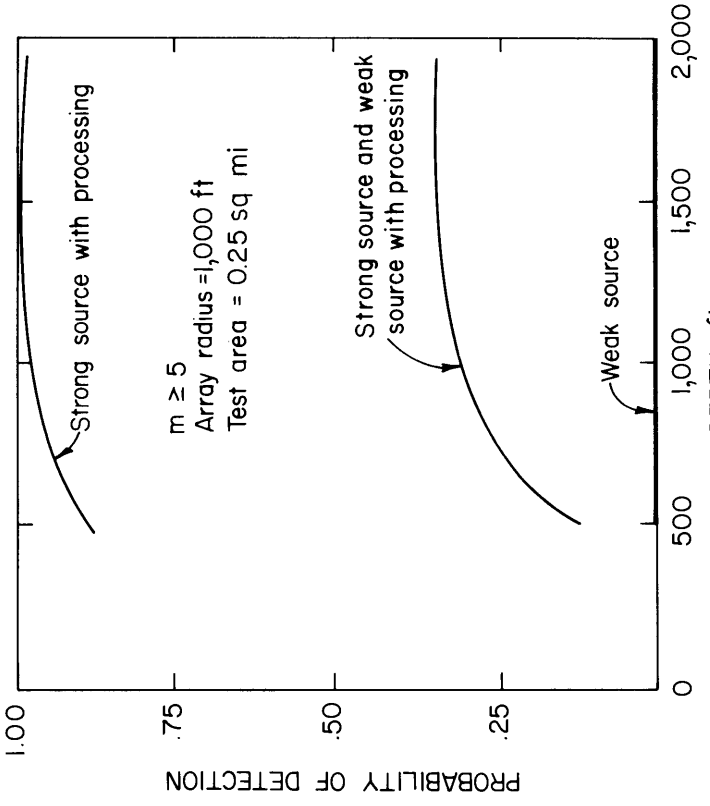

FIGURE 30. - Probability of detecting a miner's signal as a function of depth by five or more subarrays in an array of 1,000-ft radius monitoring a square area 0.5 mile on a side.

LOCATION ACCURACY

To guide the efforts of the rescue team or to determine where to site the rescue drill, it is necessary to determine the location of the trapped miner. For the rescue team an accuracy of 100 ft or less would appear desirable. For positioning the drill an accuracy of a few feet would be desirable. However, as discussed below, accuracies of a few feet do not appear feasible. Thus the positioning of a rescue drill so as to intersect a mine entry near the estimated location of the trapped miner would best be done using a mine map, if available.

The seismic system presently uses the "MINER" program (12) to calculate the location from arrival times measured on stacked seismograms. This program combines the individual subarray arrival times either three or four at a time to find a location. The MINER program can use a known depth for the source or can fit for the source depth. Alternate methods of location based on the least squares principle are more often used in seismic location work; this principle is the basis of work done by Ruths (22).

Westinghouse (24) compiled estimates of location errors obtained for a limited number of locations at 12 mines. Table 10 gives these results. This table indicates that horizontal location errors are usually below 100 ft. However, it should be understood that these results are generally for the better SNR events and that the majority of the sources were located near the center of the array where location accuracy is best.

TABLE 10. - Number of mines with average horizontal error in four ranges

Error range	Number of mines within error range
0-49 ft.....	4
50-99 ft.....	6
100-199 ft.....	2
Over 200 ft.....	0

Two of the mines discussed by Westinghouse had average errors of approximately 150 ft. In addition extensive work by Ruths (22) showed errors of this order of magnitude for Island Creek's Hamilton #1 Mine. The mines at which the larger errors occur tend to have topographic relief and geologic conditions that vary with position. Ruth's work indicates that the presence of very-low-velocity soil layers that are different between the subarrays is among the most serious sources of error.

A technique to relate location error estimates in a statistical manner to estimates of the arrival time "reading errors" was implemented. The method used is similar to that described by Crosson and Peters (5) and Peters and Crosson (20). In the location of miners the two most significant sources of errors are errors in reading arrival times in low-SNR situations and individual delays at the different subarrays caused by soil and/or water table variations. Both of these types of arrival time errors are uncorrelated between subarrays so may be treated as "reading errors."

In the present computer implementation contours are drawn of the semimajor axis of the 95-pct fiducial confidence ellipse (7). This confidence ellipse is the elliptic curve on the floor of the mine that should contain the true source location 95 pct of the time. Thus on the average the error will be somewhat less than half the semimajor axis fiducial confidence ellipse. Figure 32 shows a computer-generated contour plot for the subarray configuration used for the Hamilton #1 Mine test. The mine depth is approximately 600 ft. In generating figure 32, an rms reading error of 0.008 sec was used.

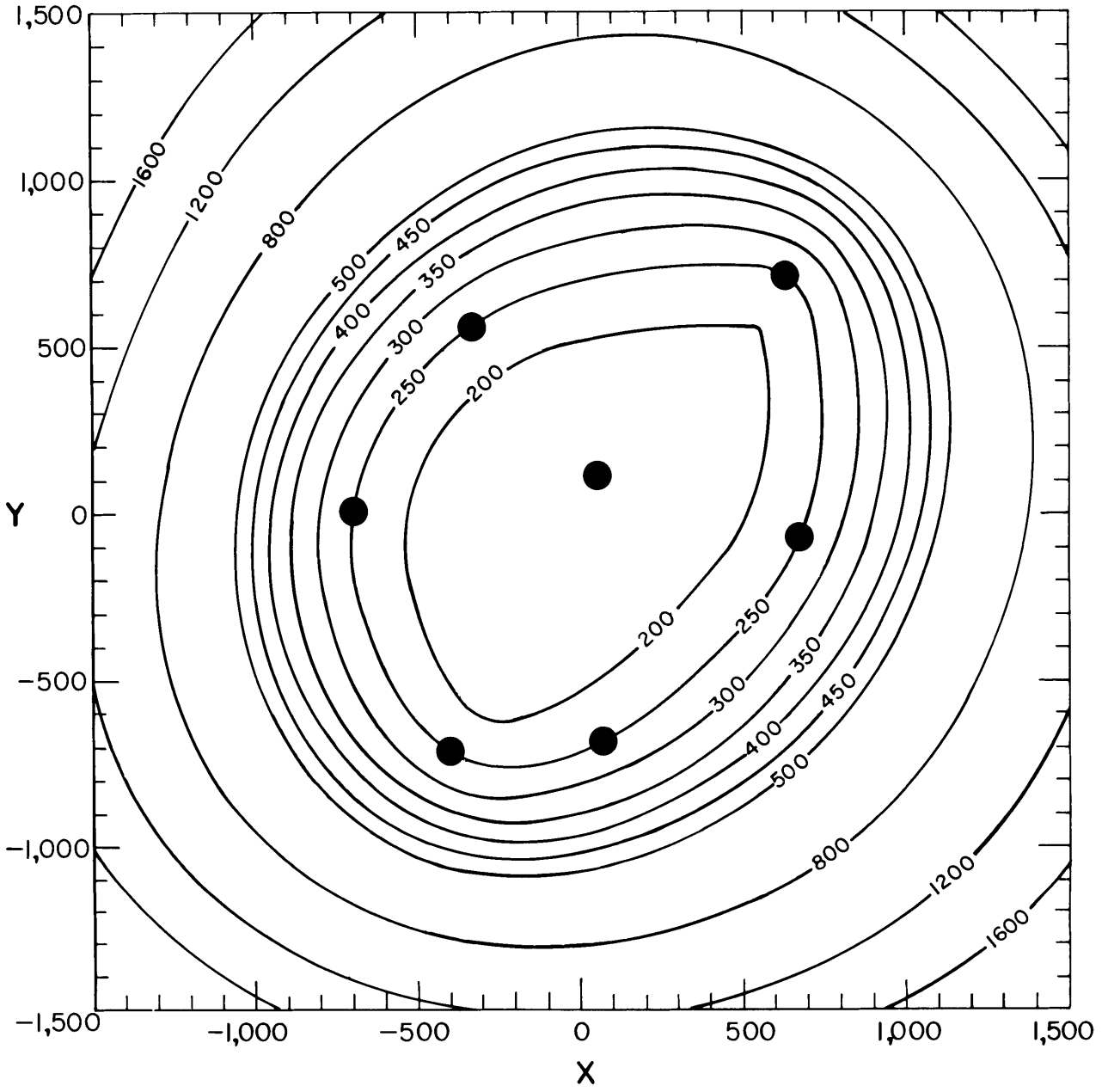

FIGURE 32. - Location error contours over area of the mine, Hamilton #1 array.

This rms reading error was used based on soil thickness variations measured at the Hamilton #1 Mine by means of a short refraction survey at each subarray location. The unsaturated low-velocity soil (1,000 ft/sec velocity) ranged in thickness from 0 to 20 ft, which gives an unaccounted-for variation in arrival times of up to 0.020 sec. Location errors up to 200 ft were observed for the test.

Three techniques have been used to decrease the location error resulting from soil layer variations. Results to date with these techniques indicate that soil-layer-related errors can be reduced to 100 ft or less. Ruths (22) studied the first of these techniques both by computer simulations and by study of data from an earlier Island Creek field test (25). In technique 1, called the Reference Correction Method, it is necessary to get a source to within a several hundred feet of the suspected position of the trapped miner. This might be impractical in a disaster situation. As an alternative method of employing technique 1, a receiver in a drill hole near the level of the mine might be used to measure travel times from shots near each subarray. The Reference-Correction Method appears to greatly improve the probability that location errors will be below 100 ft even in mines with highly variable near-surface conditions. In technique 2 a short refraction measurement is made at each subarray and used to make an arrival time correction. In technique 3 an arrival time is measured at each subarray from a blast at a known position outside the seismic array. Recent work at the Hamilton #1 Mine (March 1980) gives an indication that the errors from soil layer variations can be greatly decreased by use of technique 2 or 3.

SUMMARY

A system based upon seismic techniques, as envisioned by the National Academy of Engineering in 1970, has proven to be an effective means for detecting and locating miners trapped underground following a mine disaster.

Expected signals from miners pounding on the roof of a mine are of sufficient strength to enable detection over a large area of the mine. Estimations of the location of the trapped miner are of sufficient accuracy to aid the rescue team or the position of the rescue drill.

The seismic system, as discussed in this report, is presently operational and in a state of readiness in the event of a mine disaster. It should prove to be an invaluable aid to future postdisaster rescue efforts.

REFERENCES

1. Abramowitz, M., and I. A. Stegum. Handbook of Mathematical Functions. NBS, 1964, p. 941.

2. Bollinger, G. Blast Vibration Analysis. Southern Illinois Press, Carbondale, Ill. 1971, pp. 37-45.

3. Capon, J., R. J. Greenfield, R. J. Kolker, and R. T. Lacoss. Short-Period Signal Processing Results for the Large Aperature Seismic Array. Geophysics, v. 33, 1968, pp. 452-472.

4. Capon, J., R. J. Greenfield, and R. T. Lacoss. Long-Period Signal Processing Results for the Large Aperature Seismic Array. Geophysics, v. 34, 1969, pp. 305-329.

5. Crosson, S., and D. C. Peters. Estimates of Miner Location Accuracy: Error Analysis in Seismic Location Procedures for Trapped Miners. Part 3 in Survey of Electromagnetic and Seismic Noise Related to Mine Rescue Communications. Volume II. Seismic Detection and Location of Isolated Miners (USBM Contract HO 122026), by L. Lagace, J. J. Ginty, M. F. Roetter, R. H. Spencer, and Consultants. BuMines Open File Rept. 38 (2)-74, 1974, pp. 3.1-3.36; available for consultation at the Bureau of Mines libraries in Pittsburgh, Pa., Denver, Colo., Spokane, Wash., Twin Cities, Minn., and Morgantown, W. Va.; at the Central Library, U.S. Department of the Interior, Washington, D.C.; and from the National Technical Information Service, Springfield, Va., PB 235 070/AS.

6. Durkin, J., and R. J. Greenfield. Study of Possible Modifications to the Trapped Miner Seismic Location System. Pittsburgh Mining and Safety Research Center, Pittsburgh, Pa., Interim Report BuMines 4268, May 15, 1979, 95 pp.

7. Evernden, J., Jr. Precision of Epicenter Obtained by Small Number World-wide Stations. Bull. Seis. Soc. America, v. 59, 1969, pp. 1365-1398.

8. Feller, W. An Introduction to Probability Theory and Its Applications. John Wiley & Sons, Inc., New York, v. 1, 1950, 461 pp.

9. Frantti, G. E. Investigation of Short-Period Seismic Noise in Major Physiographic Environments of Continental United States. Prepared for the U.S. Air Force under Contract AF 19 (628-200), Task No. 865204, June 1965; available from National Technical Information Service, Springfield, Va., AD 617122.

10. _____. The Nature of High Frequency Noise Spectra. Geophysics, v. 28, 1963, pp. 547-563.

11. Futterman, W. I. Dispersive Body Waves. J. Geophys. Res., v. 67, 1962, pp. 5279-5291.

12. George, D. C., and R. F. Linfield. Seismic Subsystem Location Calculation: Software Concepts and Interpretation. Sec. in Trapped Miner Location and Communication System Development Program. V. 1. Development and Testing of an Electromagnetic Location System (USBM Contract HO 220073), by A. J. Farstad, C. Fisher, Jr., R. F. Linfield, R. O. Maes, and B. Lindeman. BuMines Open File Rept. 41 (1)-74, 1973, pp. G.1-G.23; available for consultation at the Bureau of Mines libraries in Pittsburgh, Pa., Denver, Colo., Spokane, Wash., Twin Cities, Minn., and Morgantown, W. Va.; at the Central Library, U.S. Department of the Interior, Washington, D.C.; and from the National Technical Information Service, Springfield, Va., PB 235 604.

13. Greenfield, R. Detection Range and Arrival Time Estimates. Part 3 in Survey of Electromagnetic and Seismic Noise Related to Mine Rescue Communications. V. II. Seismic Detection and Location of Isolated Miners (USBM Contract HO 122026), by R. L. Lagace, J. J. Ginty, M. F. Roetter, R. H. Spencer, and Consultants. BuMines Open File Rept. 38 (2)-74, 1974, pp. 2.1-2.30; available for consultation at the Bureau of Mines libraries in Pittsburgh, Pa., Denver, Colo., Spokane, Wash., Twin Cities, Minn., and Morgantown, W. Va.; at the Central Library, U.S. Department of the Interior, Washington, D.C.; and from the National Technical Information Service, Springfield, Va., PB 235 070/AS.

14. Greenfield, R. J. Seismic Radiation From a Point Source on the Surface of a Cylindrical Cavity. Geophysics, v. 43, 1978, pp. 1071-1082

15. Harrington, D., and W. J. Fene. Barricading as a Life-Saving Measure Following Mine Fires and Explosions. BuMines, Miners Circ. 42, 1948, 80 pp.

16. Haskell, N. A. Critical Reflection of P and SV Waves. J. Geophys. Res., v. 67, 1962, pp. 4751-4767.

17. LaCoss, R. T., E. J. Kelly, and M. N. Toksoz. Estimation of Seismic Noise Using Arrays. Geophysics, v. 34, 1969, pp. 21-38.

18. Leblanc, G. Truncated Crustal Transfer Function and Fine Crustal Structures Determination. Bull. Seis. Soc. America, v. 57, 1967, pp. 0719-0734.

19. National Academy of Engineering, Committee on Mine Rescue and Survival Techniques, Mine Rescue and Survival. BuMines OFR 4-70, March 1970, 81 pp.; available for consultation at the Bureau of Mines facilities at Denver, Colo., Minneapolis, Minn., Pittsburgh, Pa., Juneau, Alaska, and Spokane, Wash.; at the MSHA facilities at Pittsburgh, Pa., Wilkes-Barre, Pa., Johnstown, Pa., St. Clairsville, Ohio, Mount Hope, W. Va., Morgantown, W. Va., and Norton, Va.; and at the National Library of Natural Resources, U.S. Department of the Interior, Washington, D.C.

20. Peters, D. C., and Crosson, R. S. Application of Prediction Analysis to Hypocenter Determination Using a Local Array. Bull. Seis. Soc. America, v. 62, 1972, pp. 775-788.

21. Quo, J. T. Theoretical Seismic Signal Source and Transmission Characteristics. Part 7 in Survey of Electromagnetic and Seismic Noise Related to Mine Rescue Communications. V. II. Seismic Detection and Location of Isolated Miners (USBM Contract HO 122026), by R. L. Lagace, J. J. Ginty, M. F. Roetter, R. H. Spencer, and Consultants. BuMines Open File Rept. 38 (2)-74, 1974, pp. 7.1-7.33; available for consultation at the Bureau of Mines libraries in Pittsburgh, Pa., Denver, Colo., Spokane, Wash., Twin Cities, Minn., and Morgantown, W. Va.; at the Central Library, U.S. Department of the Interior, Washington, D.C.; and from the National Technical Information Service, Springfield, Va., PB 235 070/AS.

22. Ruths, M. A. The Reference-Correction Method for Improving Accuracy in the Seismic location of Trapped Coal Miners. M.S. Thesis, Pa. State Univ., Coll. of Earth and Mineral Sciences, University Park, Pa., November 1977, 141 pp.

23. Sung, T. Y. Vibrations in Semi-Infinite Solids Due to Periodic Surface Loading in Symposium on Dynamic Testing of Soils. American Society for Testing and Materials, Philadelphia, Pa., 1953, pp. 35-63.

24. Westinghouse Corp. Mine Emergency Operations Program Seismic Location Field Test Program. Report for MESA Contract JO277500, April-September, 1977; available for consultation at Pittsburgh Research Center, Bureau of Mines, Pittsburgh, Pa.

25. _____. Mine Emergency Operations Group, Field Tests--Seismic Location System. Final Report for MESA Contract J2775001, 403 pp., March-October 1976; available for consultation at Pittsburgh Research Center, Bureau of Mines, Pittsburgh, Pa.

26. Westinghouse Electric Corp. Coal Mine Rescue and Survival. V. 2: Communications Location Subsystem (USBM Contract HO 101 262). BuMines Open File Rept. 9(2)-72, 1971, 258 pp.; available for consultation at Bureau of Mines libraries at Pittsburgh, Pa., Denver, Colo., Twin Cities, Minn., and Spokane, Wash.; at the Central Library, U.S. Department of the Interior, Washington, D.C.; and from the National Technical Information Service, Springfield, Va. PB 208 267.

27. White, J. E. Seismic Waves: Radiation, Transmission, and Attenuation. McGraw-Hill Book Co., Inc., New York, 302 pp.

APPENDIX A.--RELATION OF THE AMPLITUDE DISTRIBUTION OF A NARROW-BAND NOISE ENVELOPE TO RMS LEVEL

The zero-to-peak amplitude R of the envelope of narrow-band noise is given by the Rayleigh distribution:

$$P(R) = \frac{R}{\sigma_N^2} \exp\ (-R^2/2\sigma_N^2) \qquad \text{(A-1)}$$

where σ_N is the noise rms.

With noise alone, the probability that a single measurement of the envelope amplitude R will exceed some value R_o is

$$P[R > R_o] = \exp\ (-R_o^2/2\sigma^2)\ . \qquad \text{(A-2)}$$

The equation is plotted in figure A-1. Frantti (9) gave results in terms of the P-P amplitude of the envelope. If it is assumed that the envelope value he recorded was the R_o which has a probability of being exceeded of 1/7500, the σ_N may be estimated from his data using the value

$$R_o/\sigma_N = 4.22$$

read from figure A-1.

Note that the R_o/σ_N value used is quite insensitive to large changes in probability of R exceeding R_o. For example, the value of 4.22 adopted for a probability of 1.33×10^{-4} only changes to 4.7 if a probability of 1×10^{-5} is used. If a probability of 10^{-3} has been used, the R_o/σ_N value would have been 3.7.

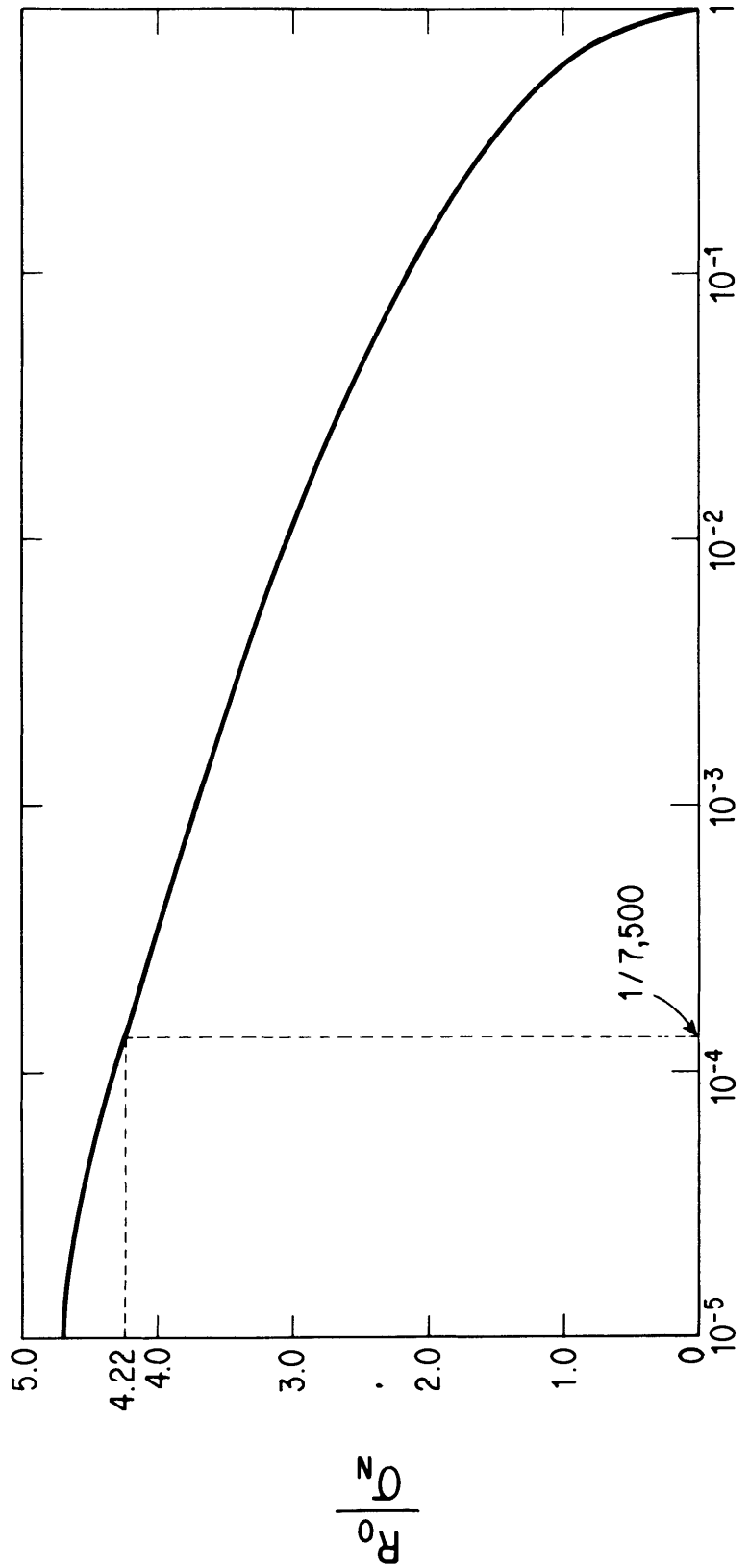

FIGURE A-1. - Probability of signal peak (R) exceeding threshold point (R_o) as a function of the ratio of R_o to the noise rms level σ_N.

APPENDIX B.--NOMENCLATURE

$A(h)$	area of mine at depth h
A_M	coefficient for amplitude model M
C	difference, in decibels
D	distance implement moves before contact
D_s	thickness of soil layer
d	decay constant
$d_R(t)$	radial displacement time history
EMI	electromagnetic interference
F	force applied to accelerate implement
f	frequency
G	force of gravity per unit mass
G_S	SNR gain of subarray
g_0	constant in force time history
g(t)	force time history of implement
h	mine depth
j	event number
k	subarray number
$\overline{k}$	wavenumber vector
k_N	horizontal wavenumber of noise
M	mass of implement
M	model number and power of cos Θ dependence
N	noise particle velocity
N	number of pulses stacked
N	number of seismometers in a subarray
N_S	number of amplitude measurements

P	implement momentum at contact
P-P	peak to peak
P_L, Q_L	cumulative distribution functions
$P_{[m]}$, P_i	probabilities
Q	quality factor for seismic wave attenuation
R	source-to-receiver distance
R_0	zero to peak detection threshold
rms	root mean square
S1	denotes type of source
SD	standard deviation
SNR	signal-to-noise ratio
$S_i(t)$	signal oM ith geophone
S_M	squared error for Mth model
S_0	signal output of a subarray
T	A_1/N, amplitude coefficient divided by noise level
t	time
V	wave velocity
Ve	ground particle velocity
V_H	horizontal phase velocity
V_p	compressional wave seismic velocity
VOL	volume of mine
WMP	waveform modeling procedure
w	angular frequency
$X_i(t)$	ith geophone output
$\overrightarrow{Y_i}$	seismometer location vector
Y(t)	subarray output

δ	degrees of freedom
ε	rebound coefficient
η_0	constant in displacement time history
$\eta(t)$	displacement time history of implement, into mine surface
Θ	angle, at source, between upward vertical and receiver
μips	microinches per second (unit of ground particle velocity)
ρ	rock density
σ_N	noise root mean square
y	horizontal offset between source and receiver
$\tau_s/2$	time implement dwells in contact with surface
χ^2	chi squared, statistical variable

☆U.S. GOVERNMENT PRINTING OFFICE: 1981-703-002/82 INT.-BU.OF MINES,PGH.,PA. 25552